Targeting Chemotherapy-Induced Senescence Escape to Reduce Breast Cancer Cell Survival

Danlin Zeng

Department of Biochemistry, McGill University

February 2023

A thesis submitted to McGill University in partial fulfillment of the requirements of the degree of Master of Science

Table of Contents

Abbreviations

AEBSF	4-(2-aminoethyl)benzenesulfonyl fluoride hydrochloride
ATM	Ataxia-Telangiectasia Mutated
ATR	ATM and RAD3-related
BRCA	Breast Cancer Gene
CDK	Cyclin Dependent Kinase
CHK	Checkpoint Kinase
DCA	Dichloroacetate
DMEM	Dulbecco's Modified Eagle's Medium
DNA	Deoxyribonucleic Acid
EDTA	Ethylenediaminetetraacetic Acid
EGF	Epidermal Growth Factor
ER	Estrogen Receptor
FBS	Fetal Bovine Serum
HCl	Hydrochloric Acid
HER2	Human Epidermal Growth Factor Receptor 2
IL	Interleukin
mTOR	Mammalian Target of Rapamycin
NACT	Neoadjuvant Chemotherapy

NaF	Sodium Fluoride
NaPP	Sodium PyroPhosphate
PALB	Parvalbumin
PBS	Phosphate Buffered Saline
pCR	Pathological Complete Response
PDK	Pyruvate Dehydrogenase Kinase
PDX	Patient-Derived Xenograft
PR	Progesterone Receptor
RIPA	Radioimmunoprecipitation Assay
RNA	Ribonucleic Acid
ROCK	Rho Kinase
RPM	Revolutions Per Minute
SA-β-gal	Senescence-Associated Beta-Galactosidase
SAHF	Senescence-Associated Heterochromatin Foci
SASP	Senescence-Associated Secretory Phenotype
SB	Sample Buffer
SDS	Sodium Dodecyl Sulfate
TBS	Tris-Buffered Saline
TBST	Tris-Buffered Saline + 0.1% Tween

TNBC	Triple-Negative Breast Cancer
WGS	Whole Genome Sequencing
2-DG	2-Deoxy-D-Glucose

Abstract

Breast cancer is the most frequently diagnosed cancer worldwide. For certain subtypes of breast cancer that lack effective targeted therapy, there is a higher chance of cancer recurrence within three years after chemotherapy. DNA-damaging agents such as cisplatin are widely used in the clinic as chemotherapy, and while cisplatin is highly effective initially in shrinking breast tumors, there is a high chance of relapse following cisplatin treatment. Previous studies have suggested that while acute cisplatin exposure does induce tumor cells to undergo apoptosis, some cancer cells temporarily enter a reversible state of senescence instead. Certain senescent cells may re-enter proliferation in the off-treatment periods and may be partially responsible for cancer recurrence. Our data show that breast cancer cells treated briefly with cisplatin become senescent and are more selectively eliminated by senolytic drugs targeting senescent cells, such as navitoclax, phenformin, and rapamycin. Our findings suggest that breast cancer patients with a high recurrence risk following standard of care DNA-damaging chemotherapy could benefit from receiving an additional senolytic drug following chemotherapy. Based on the data from this preclinical study, our aim is to determine which drug combinations may reduce cancer cell re-growth by selectively targeting the cells responsible for re-growth.

Résumé

Le cancer du sein est le cancer le plus fréquemment diagnostiqué dans le monde. Pour certains sous-types de cancer du sein dépourvus de traitement ciblé efficace, le risque de récidive du cancer est plus élevé dans les trois ans suivant la chimiothérapie. Les agents endommageant l'ADN tels que le cisplatine sont largement utilisés en clinique comme chimiothérapie, et bien que le cisplatine soit initialement très efficace pour réduire les tumeurs du sein, il existe un risque élevé de rechute après un traitement au cisplatine. Des études antérieures ont suggéré que si l'exposition aiguë au cisplatine incite les cellules tumorales à subir l'apoptose, certaines cellules cancéreuses entrent plutôt dans un état réversible de sénescence. Cette population de cellules sénescentes peut entrer à nouveau en prolifération dans les périodes hors traitement et peut être en partie responsable de la récidive du cancer. Nos données montrent que les cellules cancéreuses du sein traitées brièvement avec le cisplatine deviennent sénescentes et sont éliminées plus sélectivement par des médicaments ciblant les cellules sénescentes, tels que le navitoclax, la phenformine et la rapamycine. Nos résultats suggèrent que les patientes atteintes d'un cancer du sein présentant un risque élevé de récidive après une chimiothérapie standard endommageant l'ADN pourraient bénéficier de l'administration d'un médicament supplémentaire après la chimiothérapie. Sur la base des données de cette étude préclinique, nous serons en mesure de déterminer quelles combinaisons de médicaments peuvent réduire la régénération des cellules cancéreuses en ciblant sélectivement les cellules responsables de la régénération.

Contribution of authors

All the assays (except Figure 3A, which was performed by Dr. Anne-Marie Fortier) were performed by me. I received supervision and assistance from Dr. Anne-Marie Fortier.

Acknowledgements

This research was funded by a grant from the Cancer Research Society. The work presented in this thesis was performed under the supervision of Dr. Morag Park and Dr. Anne-Marie Fortier. Dr. Hellen Kuasne and Dr. Anne-Marie Fortier generated the PDX-derived cell lines utilized in this thesis.

I want to thank Dr. Anne-Marie Fortier, who has served as my mentor from my first day in the lab. Thank you for being so patient with me and for encouraging me, always. You are an amazing mentor, and I could not have accomplished so much without you. You have shown me what an amazing mentor is like. You are an inspiration to the life I will lead. Thank you, Dr. Morag Park, for always being honest with me and being a big source of motivation for me during difficult times. I really appreciate all the feedback and advice you gave me.

I want to thank everyone in the Park Lab for welcoming me and for showing me the value in collaboration. I look forward to hearing about all your achievements in the future, whether personal or professional. To all students in the Goodman Cancer Student Society (GCSS), thanks for building a strong sense of community and allowing me to feel part of something bigger than myself.

To Julie Gan, thank you for supporting my ambitions and encouraging me to follow my dreams. To Serena Wu, I will forever remember the support you showered me with, on the many days I felt overwhelmed and directionless. To Lucie Barthelemy, I miss you being such a ray of sunshine. To Adéline Massé and Alice Nam, I will always cherish the late nights and weekends

we spent together in the lab. I can't wait to hear about what you guys accomplish in your PhDs – I am so proud of you both. To Thomas MacDonald, Raymond Shi, Jenny Liu, Cherry Tang, and Arlene So, I love that I can always have meaningful, deep conversations with you guys. You guys inspire me to be a better person every day. Most of all, to every single one of my friends reading this, just know that you have made my life so much fuller. You are the family that I chose for myself since I never had a "traditional" family. You have shown me what love is.

1. Introduction

1.1 Breast cancer

Breast cancer was the most frequently diagnosed cancer worldwide in 2022 (1). In the United States, breast cancer is the second highest cancer-related cause of death for women (2). In the recent few years, breast cancer incidence rates have increased steadily by 0.5% every year, partially attributable to the advancements made in breast cancer screening methods. In 2022, around 28,600 cases of breast cancer were diagnosed in Canada, with approximately 5,500 women passing away from breast cancer (3). Every day, 78 women are diagnosed with breast cancer, and 15 women die from breast cancer in Canada (4). It was estimated that approximately one in eight women will develop invasive breast cancer at some point in their lifetime, and 1 in 39 women will die from breast cancer (5). Though rare, it is also possible for men to develop breast cancer. In 2022, approximately 270 men were diagnosed with breast cancer in Canada, with nearly 60 deaths from their cancer (4). Every year, nearly 2,600 men are diagnosed with male breast cancer in the United States.

Aging is a risk factor for breast cancer, as most breast cancers are diagnosed in women over the age of 55 (6). Having a first-degree family member diagnosed with breast cancer nearly doubles a woman's risk of developing breast cancer herself. The most observed mutation in hereditary breast cancer is a BRCA1 or BRCA2 mutation, though inherited mutations in other genes such as TP53, PTEN, ATM, CHEK2, also increase the risk of breast cancer (7). For women with a BRCA1 or BRCA2 mutation, the lifetime risk of developing breast cancer is approximately 50%, making genetic predispositions another very important risk factor for breast cancer. Another gene known as PALB2 is also commonly mutated in breast cancer. The PALB2 gene is the partner and localizer of the BRCA2 gene.

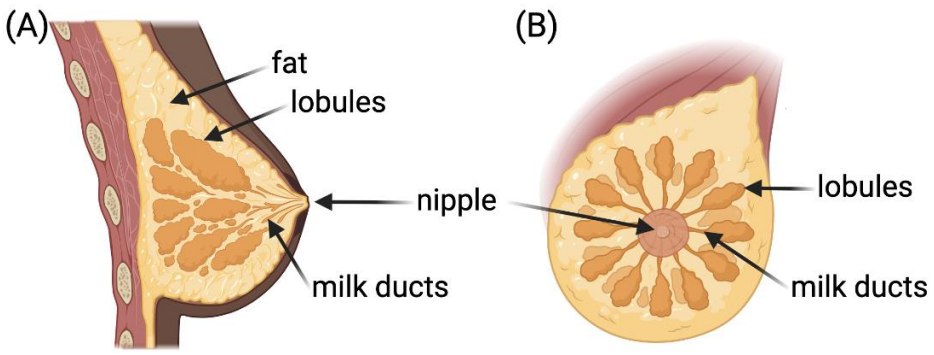

Figure 1. Anatomy of a human breast. (A) Sagittal / side view. (B) Anterior / frontal view. Most breast cancers originate from cells within milk ducts or lobules, though it is also possible for breast cancer to originate from fat tissue in the breast. Created with BioRender.com.

Breast cancer is a disease in which cells in the breast tissue divide uncontrollably, creating a mass of tissue called a tumour. There are different types of breast cancers depending on the cell origin from which the cancer arose. Breast cancer can be classified as either carcinomas or sarcomas. Carcinomas are breast cancers arising from the epithelial components of the breast, which consists of the cells lining the lobules and milk ducts (8). Sarcomas arise from the stromal components of the breast, which include myofibroblasts and blood vessel cells, and are much rarer (8). Most breast cancers (>99%) are carcinomas. Most breast cancers originate from milk ducts or lobules, though it is also possible for breast cancer to originate from fat tissue in the breast (5). Depending on the carcinomas' invasiveness, breast cancer can be either non-invasive (also known as in situ), invasive, or metastatic (8, 9). Non-invasive carcinoma, also known as ductal carcinoma in situ or intraductal carcinoma, develops when ductal cells in the breast divide uncontrollably but do not invade into surrounding tissue. In situ carcinomas have the potential to become invasive in the future (9). Therefore, it is beneficial to eradicate cancer before it acquires aggressive characteristics and becomes invasive. Yet, it is very challenging to do so in patients because more aggressive treatment options tend to result in

more debilitating side effects and long-term consequences. Invasive carcinomas can be further divided into either invasive ductal carcinoma or invasive lobular carcinoma (8, 9). Invasive ductal carcinoma begins when cells lining the milk-producing ducts grow and invade into the surrounding tissue. Invasive lobular carcinoma begins when lobules proliferate out of control and invade into the surrounding tissue.

The most common staging system for breast cancer divides breast cancer into five different stages—stage 0 followed by stages 1 to 4 (10). Staging depends on the size of the tumour, the biomarkers present, and whether the cancer has spread to the lymph nodes or other parts of the body (10). The higher the breast cancer stage, the more the cancer has spread for the patient (10). Stage 0 breast cancer refers to non-invasive cancers. Breast cancer cells can also travel to other parts of the body and form new tumours at new locations. This process is termed metastasis. Metastatic breast cancer is classified as Stage 4 breast cancer, the most advanced stage. Breast cancer metastasis occurs when breast cancer cells break away from their primary site and enter either the bloodstream or the lymphatic system. Breast cancer tends to travel first to the patient's underarm lymph nodes, which are close in proximity to the original tumour location. When breast cancer metastasizes, it most commonly metastasizes to the bones, liver, brain, and lungs, although it is also possible for breast cancer to metastasize to other organs (11). Over 50% of Stage 4 breast cancer patients have bone metastasis (12).

Breast cancer is clinically classified based on the presence or absence of the estrogen receptor (ER) and progesterone receptor (PR), as well as human epidermal growth factor receptor 2 (HER2) expression levels (13). Breast cancer is a heterogeneous disease that manifests differently even among different patients with the same clinical subtype of breast cancer, necessitating further classification of breast cancer. There is a significant amount of molecular heterogeneity that exists within each clinical subtype of breast cancer, leading to breast cancer

being divided into 5 intrinsic molecular subgroups, which are luminal A, luminal B, basal-like, normal-like, and HER2-enriched (13, 14). Luminal A breast cancers are ER positive and PR positive, but HER2 negative (14, 15). Luminal A breast cancers are likely to benefit from hormone therapy targeting ER or PR. Luminal B breast cancers are ER positive, HER2 positive, but negative for PR (14, 15). Triple-negative breast cancer (TNBC) is a subtype of breast cancer that does not express any of the receptors commonly found in breast cancer, such as ER, PR, and HER2. TNBC is more difficult to treat in the clinic because of its lack of therapeutic targets, and TNBC is more likely to recur than other subtypes of breast cancer (13). TNBC is a rare type of breast cancer that accounts for only 10% to 20% of all breast cancers, yet 80% of basal-like breast cancers are TNBC (13).

1.2 Standard neoadjuvant chemotherapy

Cisplatin is a widely used anticancer drug that crosslinks with the purine bases in DNA, causing DNA damage to accumulate within cells (16). This crosslink ultimately interferes with cell division by mitosis and leads to apoptosis activation in cells. Cisplatin is used to treat many different types of cancer, including bladder, ovarian, cervical, head and neck, esophageal, and breast (17). An estimated 50% of all cancer patients are treated with cisplatin, either as monotherapy or in combination with other chemotherapeutic agents, radiotherapy, or immunotherapy (18).

Neoadjuvant chemotherapy (NACT) is systemic therapy offered to patients prior to surgical resection of the tumour. Patients who have large or locally advanced tumours greatly benefit from NACT. NACT has been shown to improve disease-free survival and overall survival in patients who have a pathologic complete response (19). Thus, NACT is considered the standard approach to treat breast cancer patients with a high risk of tumour recurrence, such

as TNBC patients. NACT shrinks large tumours, prevents metastases, and can be used to evaluate chemo-efficacy. Any invasive breast cancer that remains in the breast tissue or axillary lymph nodes after neoadjuvant chemotherapy is termed residual breast cancer (20). Multiple researchers have shown that achieving pathological complete response (pCR) after NACT is associated with better prognosis (20, 21). Following neoadjuvant chemotherapy, breast cancer patients with any sign of residual disease are at a higher risk for relapse (22). Patients with a smaller-volume residual disease were seen to have longer overall survival.

1.3 Breast cancer recurrence

Breast cancer recurrence means the same breast cancer began re-proliferating after a period of time in which the patient showed no signs of cancer. For many patients, breast cancer returns after treatment, sometimes even years later. Patients with ER positive breast cancer remain at risk for distant recurrences for the remainder of their lives. Nearly half of ER positive breast cancer recurrences occur more than five years after the initial diagnosis (23, 24). Although treatment advances and the use of mammograms for earlier detection through screening has significantly decreased breast cancer mortality rates and reduced treatment morbidity, cancer relapse remains a primary concern for many patients (25).

Although many cancer patients initially show high responsiveness to cisplatin-based chemotherapy, many will relapse later with cisplatin-resistant disease. Cancer cells may exist in a dormant state for years, sometimes even decades, before recurring as a metastatic tumour (26). A study following breast cancer survivors found that breast cancer recurrences continued to occur up to 39 years after the patient's primary cancer diagnosis (27, 28). This may be explained by the fact that around 75% of breast cancer patients have micro-metastases at the time of clinical diagnosis and that these micro-metastases remain in a dormant state until factors in the

tumour microenvironment prompt their re-proliferation (29). An extended latency period was more commonly associated with larger breast tumours and higher-grade disease (23).

1.4 Senescence

Cellular senescence was defined for many years to be a state of irreversible cell cycle arrest that occurs after a finite number of cellular divisions (30). Hayflick found that cells eventually ceased dividing in culture after a finite number of cell divisions (30). Although originally observed by Hayflick in human fibroblast cells, it was later found to occur in many different cell types. Hallmarks of senescence include a flattened and enlarged cell shape, expanded lysosomes and vacuoles, increased metabolic rate and reactive oxygen species (ROS) production, secretion of pro-inflammatory factors, nuclear and chromatin alterations, and resistance to apoptosis (31).

Senescent cells resist apoptosis and persist for prolonged periods of time under the growth-arrested state. Previous studies have shown that cellular senescence can be induced with DNA-damaging drugs (32). The DNA damage response is mediated by the activation of ATM and ATR, both of which are kinases. The activation of ATM and ATR leads to the phosphorylation of downstream kinases CHK1 and CHK2, which subsequently phosphorylates and activates p53 (30, 33). Although both ATM and ATR orchestrate the DNA damage response in response to any DNA damage or DNA replication stress, these kinases do not serve redundant functions (33). p53 is a transcription factor that activates transcription of its target genes, thereby activating many different signaling pathways such as growth arrest, DNA-damage repair, and apoptosis (34). Notably, the chronic activation of p53 leads to cellular senescence. p53 binds to the promoter sequence to activate the transcription of p21, resulting in increased levels of p21. p21 is a cyclin-dependent kinase inhibitor that blocks cell cycle progression (35). DNA damage–

induced growth arrest in senescent cells is largely mediated by the activation of the p53/p21 pathway (36).

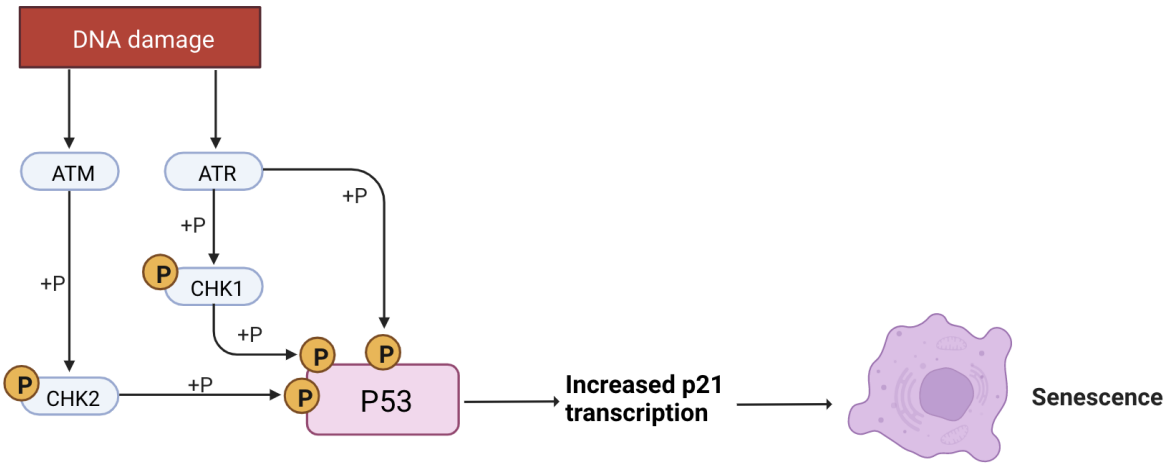

Figure 2. Activation of the p53/p21 pathway in response to DNA damage. p53 is a transcription factor that activates transcription of its many target genes, including p21, thereby inhibiting cell cycle progression and leading to growth arrest. Created with BioRender.com.

On the other hand, replicative senescence occurs following an increase in p16 expression. p16-mediated senescence acts through the retinoblastoma (Rb) pathway. Progression from G1 to S phase is tightly regulated by the p16/Rb pathway (37). Active p16 binds to CDK4/6, inhibiting its kinase activity, which subsequently prevents Rb from getting phosphorylated. When Rb is not phosphorylated, it associates with the transcription factor E2F1, suppressing the transcription of E2F1 target genes, which ultimately leads to G1 cell cycle arrest (37). p16 also appears to play a role in the maintenance of cellular senescence, as the p16/Rb pathway increases reactive oxygen species (ROS) production (38). Both intracellular and extracellular increases in ROS production have been shown to contribute to senescence induction and maintenance (33). Reactive nitrogen species, which are nitric oxide-derived compounds that have been shown to increase during the aging process, generate consequences similar to ROS (33, 39).

Cellular senescence is different from quiescence, which is another form of cell cycle arrest (Fig. 3). Quiescent cells resume proliferation when stimulated by growth factors while senescent cells do not (40). In other words, quiescence occurs due to lack of growth factors in the microenvironment, but senescence occurs in response to serious DNA damage. During the quiescent phase, the cell is neither dividing nor preparing to divide. In quiescence, cells are arrested in the G0 phase of the cell cycle, whereas senescent cells are arrested in the G1, G1/S, or G2 phases (41). Whether a cell enters senescence versus quiescence is governed to a certain extent by the mTOR pathway. Inhibition of mTOR through maximal p53 activation causes cells to enter quiescence, whereas when mTOR activity is sustained through partial p53 activation, cells become senescent instead (41).

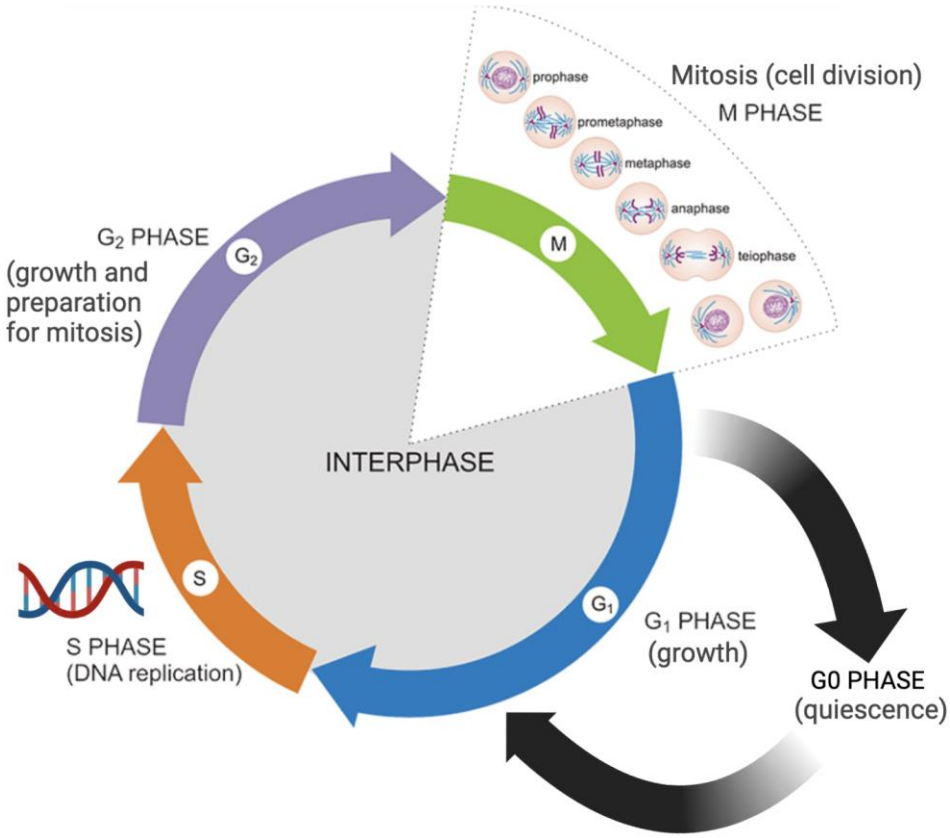

Figure 3. Different phases of the cell cycle. The cell cycle consists of G1, S, G2, and M phase. The G1 phase is when cells do most of their growing, increasing in cellular size, synthesizing new proteins and organelles. The G1 phase is followed by the S phase. During the S phase, cellular DNA and chromosomes are replicated. After the S phase, cells then enter the G2 phase, where cells prepare for cell division by synthesizing additional organelles and proteins. The M phase is when cells undergo mitosis. The G0 phase is the quiescence phase in which cells are neither dividing nor preparing to divide, also known as the resting phase. Created with BioRender.com.

One characteristic that distinguishes a senescent cell from quiescent cells that are also under cell cycle arrest is the release of SASP factors. Senescence has been termed a double-edged sword in cancer because of the many opposing roles these SASP factors may play in tumour progression. Originally, cellular senescence was thought to act as a potent tumour-suppressive mechanism that limits the proliferation of damaged cells at risk for malignant transformation (42). Since senescence occurs in response to DNA damage, senescence was believed to suppress cancer development. Through the secretion of inflammatory SASP factors, senescent cells may provide a persistent signal of oncogenic stress to facilitate immune clearance of any cells at risk of becoming cancerous (42). However, these same SASP factors secreted by senescent cells can stimulate cancer growth and promote tumour invasion by initiating inflammatory responses (43). Prolonged inflammation creates an environment that is conducive to DNA mutations, tissue damage, and eventual cancer development (43, 44). Many cancers arise from sites of chronic inflammation (44). In conclusion, recent literature suggests that cellular senescence may have dual effects on tumour progression (Fig. 4).

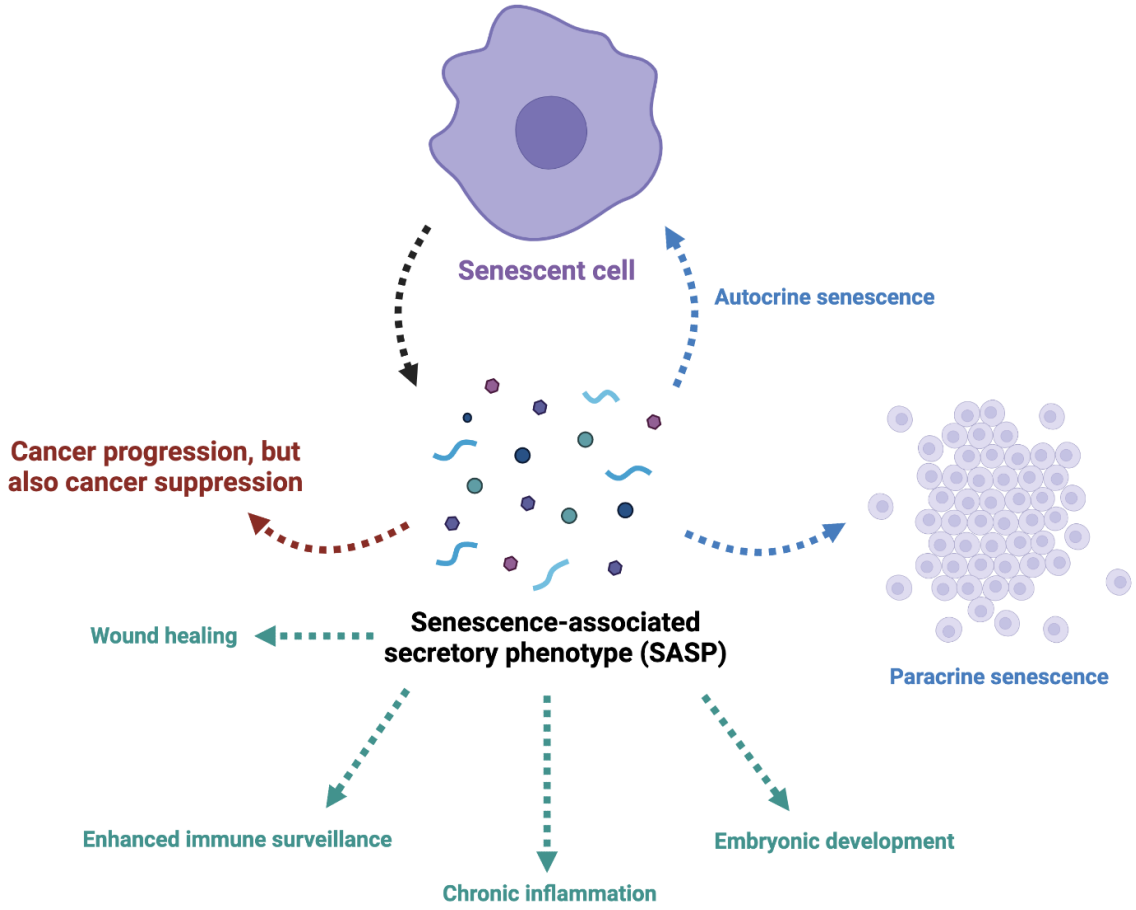

Figure 4. The senescence-associated secretory phenotype (SASP) released by senescent cells serves many roles. SASP factors are known to be involved in immune cells recruitment, chronic inflammation, healing of wounds, tumour-suppression, but also cancer progression. SASP factors also reinforce the senescent state of the cell while also inducing neighbouring cells to enter senescence. Created with BioRender.com.

1.5 Characteristics of senescent cells

Senescent cells can be distinguished from non-senescent cells by its increased and irregular cell shape, darker nuclear chromatin, increased lysosomal content, increased metabolic rate due to mitochondrial accumulation, enlarged endoplasmic reticulum, enlarged vacuoles, senescence-associated secretory phenotype (SASP), and resistance to cell death (45). Higher

levels of lysosomal content in senescent cells may result from the accumulation of cellular damage, therefore requiring higher levels of degradative capacity within the cell. Increased levels of degradation within senescent cells may also explain the increase in vacuole size. The endoplasmic reticulum is where the synthesis and folding of membrane and secretory proteins occurs, and an enlarged endoplasmic reticulum allows more time for misfolded proteins to be folded correctly. Thus, the endoplasmic reticulum enlarges primarily in response to cellular stressors, helping the cell survive.

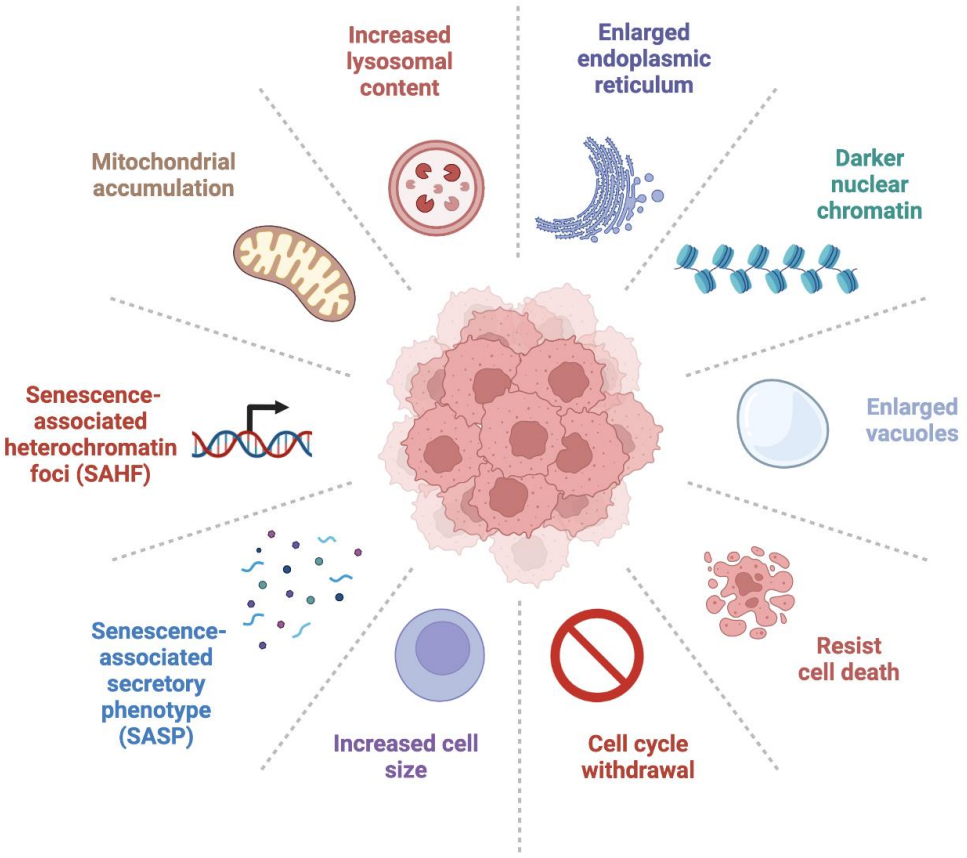

Figure 5. Hallmarks of senescent cells. Hallmarks of senescent cells include mitochondrial accumulation, increased lysosomal content, enlarged endoplasmic reticulum, darker nuclear chromatin, enlarged vacuoles, apoptosis resistance, cell cycle withdrawal, enlarged and irregular cell size, a senescence-associated secretory phenotype (SASP), and a senescence-associated heterochromatin foci (SAHF). Created with BioRender.com.

One characteristic observed in senescent cells is the formation of highly dense heterochromatin senescence-associated heterochromatin foci (SAHF) domains (46, 47). SAHFs are specific to senescent cells and not associated with cells undergoing quiescence. Chromatin is the compact package of DNA and protein found within a cell's nucleus, with more tightly condensed forms of chromatin indicating DNA that is less transcribed. Tightly condensed chromatin is also known as heterochromatin, and SAHF formation is observed in senescent cells (47). SAHF suppresses the expression of proliferation-promoting genes by rendering promoter regions inaccessible to transcriptional machinery (46). Therefore, SAHF formation eliminates any active transcription sites in the DNA. Most notably, the promoter region of E2F target genes, including cyclin A, acquire SAHF formation in senescent cells. E2F target genes such as cyclin A are necessary for cell cycle progression (48).

In addition to SAHF, senescent cells also display a SASP, which consists of growth factors, inflammatory chemokines, proteases, and extracellular matrix components (49). SASP factors have many paracrine effects on neighbouring cells. SASP has been shown to affect the tissue microenvironment in many ways that promote tumour progression (49). SASP is thought to allow damaged cells to communicate their state to nearby cells and mobilize the immune system for their clearance. Other studies have suggested that the secretion of inflammatory factors contributes to tumour progression and metastasis in neighbouring cells (42). Interleukin-6 (IL-6) is the most prominent cytokine secreted by senescent cells. IL-6 exerts its pro-inflammatory effects through binding to cell-surface receptors on nearby cells (50). Among the many SASP factors, IL-1, IL-8, and colony-stimulating factors (CSF) are the notable ones that also initiate inflammatory responses in neighbouring cells (49). Interestingly, senescent cells that are induced by different stress stimuli have been shown to secrete different SASP factors (51).

In a laboratory, senescent cells can be detected via several methods. Firstly, the flattened and enlarged morphology of senescent cells is easily detectable under a microscope. Second, SA-β-gal staining detects activity of the lysosomal enzyme, SA-β-gal, that is abundant only in senescent cells. SA-β-gal activity is the most widely used marker of senescence. The other signature changes associated with senescence include an increase in p21 levels and a decrease in Lamin B1 levels.

Lamin B1 is an intermediate filament protein encoded by the LMNB1 gene. Lamin B1 is a major structural component of the nuclear lamina. Due to its ability to provide stability and structure to the nucleus, Lamin B1 is thought to be involved in maintaining nuclear stability and the regulation of nuclear functions, chromatin structure, and gene expression (52). Lamin B1 loss is associated with multiple types of cellular senescence, including DNA damage-induced senescence, oncogene-induced senescence, and replicative senescence (53). Lamin B1 does not decline in quiescent cells, thus making it a specific marker for senescent cell cycle arrest (53).

1.6 Senolytic drugs

Senolytic drugs are drugs that selectively eliminate senescent cells. Different senolytic drugs can target senescent cells via various mechanisms, including the mitochondrial accumulation or the increased expression of anti-apoptotic proteins.

Table 1: Senolytic drugs and their mechanism of action.

Senolytic drug	Mechanism of Action	Pathways affected
Navitoclax	Inhibits BCL-2 family proteins, which includes BCL-XL, BCL-2, and BCL-W	Anti-apoptotic pathway inhibited, subsequently leading to apoptosis
Phenformin	Inhibits complex I of the mitochondrial respiratory chain	Electron transfer chain inhibited
Rapamycin	Inhibits mTOR	mTOR pathway inhibited
2-DG	Glucose analogue that inhibits glycolysis	Glycolysis inhibited
DCA	Acetic acid analogue that inhibits the enzyme pyruvate dehydrogenase kinase	Glycolysis inhibited

Navitoclax, also known as ABT-263, is one of the first senolytic drugs to be discovered. Navitoclax has been proven to eliminate a wide range of senescent cell types, including senescent hematopoietic stem cells, neural precursor cells, muscle stem cells, and mesenchymal stromal cells (54). To date, it remains one of the most well-researched senolytic compounds. Navitoclax exerts its senolytic effects through inhibiting BCL-2 family proteins including BCL-XL, BCL-2, and BCL-W (54). BCL-2 family proteins are anti-apoptotic, thus inhibiting BCL-2 family proteins causes cells to activate the intrinsic apoptosis mechanism (54, 55). Senescent cells upregulate the anti-apoptotic proteins BCL-W and BCL-XL within the BCL-2 family of proteins. Thus, the inhibition of BCL-2 family proteins directs senescent cells specifically to undergo apoptosis.

On the other hand, phenformin is a drug that inhibits complex I of the mitochondrial respiratory chain (56). Phenformin interferes with the electron transfer chain, leading to the production of reactive oxygen species, which eventually leads to apoptosis activation (56). Senescent cells have a significantly increased mitochondrial size, thus they rely more heavily on oxidative phosphorylation for energy generation and survival. Thus, inhibition of complex I in

the mitochondria has been shown to selectively remove senescent cells with dysfunctional mitochondria and high metabolic activity.

Rapamycin, also known as sirolimus, inhibits the mTOR signaling pathway. Recent studies have shown that prolonged activation of the mTOR pathway is closely associated with growth arrest and cellular senescence (57). Recent literature has suggested that inhibition of the mTOR signaling pathway using rapamycin leads to an increase in lifespan (58). Though there is evidence supporting the fact that mTOR inhibition increases lifespan, the mechanism by which mTOR regulates lifespan remains uncertain. Researchers have hypothesized that mTOR inhibition may exert its effects on lifespan through delaying age-related disorders, which are brought upon by senescent cells (58). Rapamycin is currently the only known pharmacological treatment that prolongs lifespan in all model organisms studied, including mammals (58).

2-deoxy-D-glucose (2-DG) is a glucose analogue that replaces the 2-hydroxyl group of D-glucose with a hydrogen molecule, thus preventing glycolysis from taking place (59). 2-DG inhibits glycolysis by competing with glucose molecules to bind hexokinase, which is the first enzyme involved in glycolysis (60). Studies have shown that 2-DG leads to breast cancer cell death in a dose dependent manner (61). Dichloroacetate (DCA) is an analogue of acetic acid, with the methyl group's hydrogen atoms replaced with chlorine atoms (62). DCA inhibits the enzyme pyruvate dehydrogenase kinase (PDK), which directs cells into using oxidative phosphorylation to generate energy instead of glycolysis (62). Although there is a growing body of evidence suggesting that DCA may be promising in cancer therapy in combination with other chemotherapy agents or radiotherapy, DCA is not yet under clinical use (63).

The potential efficacy of both 2-DG and DCA in cancer therapy results from the very well-known Warburg effect, where tumour cells rely heavily on glycolysis instead of oxidative

phosphorylation to generate energy even under aerobic conditions (64, 65). As a result, high levels of glucose are needed for tumour cells to generate energy and support their metabolic activity (64, 65). Senescent cells have been shown to preferentially undergo glycolysis instead of oxidative phosphorylation even in the presence of high oxygen levels, similar to tumour cells that demonstrate the Warburg effect.

1.7 Breast cancer cell lines

There are many commercially available breast cancer cell lines. The various established breast cancer cell lines harbor different mutations and phenotypes. The MDA-MB-231 cell line chosen for this preclinical model is currently one of the most widely used breast cancer cell lines for modeling advanced late-stage breast cancer (66). The MDA-MB-231 cell line is an epithelial-like, human breast cancer cell line that is highly invasive (66). MDA-MB-231 cells are poorly differentiated and lack ER, PR, and HER2 expression, which renders MDA-MB-231 a more difficult to treat cancer because of the lack of targeted therapy available (67).

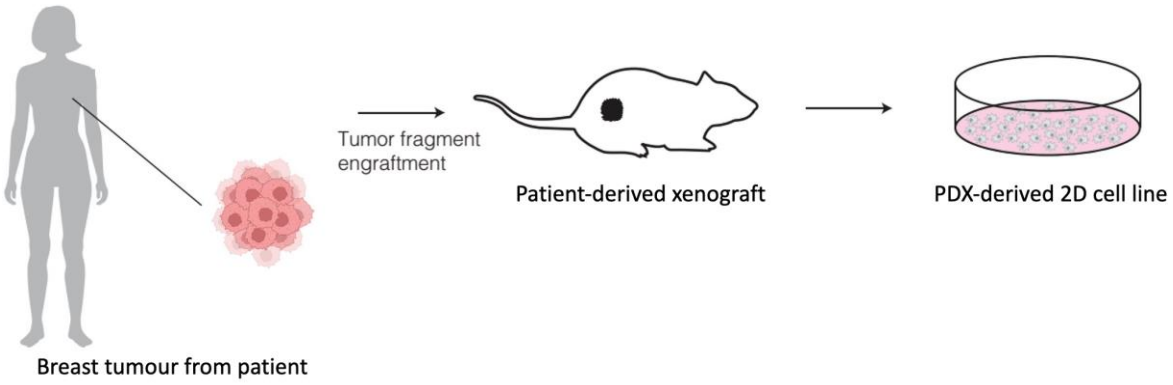

Figure 6. Generation of patient-derived xenografts (PDX) and PDX-derived 2D cell lines from a patient tumour. The breast tumour from the patient is surgically removed and a small fragment of the patient tumour is engrafted into the mammary fat pad of a non-SCID immunocompromised female mouse. Created with BioRender.com.

Translational research relies on accurate preclinical models as approximations of human tumours to advance our understanding of cancer biology. Patient-derived xenografts (PDX) are preclinical models widely used to study many different types of cancer (68). Breast cancer PDX are generated by engrafting breast cancer primary tumours fragments into the mammary fat pad of a non-SCID immunocompromised female mouse (Fig. 2). After several weeks or months, the mouse then grows a tumour that is representative of the patient's primary tumour. PDX are extensively used in research because of its ability to capture the original biology of the parental tumour from which it is developed, including its molecular and phenotypic features (68).

Dr. Park's laboratory has previously generated novel xenografts for difficult-to-treat breast tumours with inter- and intra-tumour heterogeneity. These breast cancer PDX models conserved the mutational load, copy number profiles, driver alterations, and most importantly, the therapeutic response observed in the patients (68). Our lab has performed the molecular and genomic characterization of ~35 PDX–primary tumour pairs through whole-genome sequencing (WGS), RNA sequencing (RNA-seq), reverse-phase protein array (RPPA), and in vivo

evaluation of metastatic dissemination and chemo-sensitivity (68). The 2D breast cancer cell lines derived from PDX tumours, GCRC1863, GCRC1887, GCRC1915, were utilized for in vitro assays.

1.8 Hypothesis and rationale

Other preclinical cancer xenograft models have demonstrated that combination therapy of a therapy that induces senescence with an additional senolytic can effectively reduce tumour burden (69). This combination therapy would selectively eliminate cancer cells through synergy. Cellular senescence is a potential mechanism by which chemoresistance arises in breast cancer, implying that inducing cancer cells to become senescent and then targeting that cell population with a senolytic is a promising strategy (69).

Our hypothesis is that senescent breast cancer cells may escape senescence and re-enter proliferation during off-treatment periods following chemotherapy. Although earlier studies have postulated that senescence is an anti-cancer mechanism, the ability of senescent cells to resist apoptosis and eventually re-enter proliferation upon removal of the stressor may contribute to cancer progression. Hayflick's paper claimed in 1965 that escape from senescence can only occur in cells that have properties of cancer cells (30). Despite decades of research into senescence, senescence escape has yet to be defined in many different types of cancer. If cellular senescence and eventual senescence escape contributes to cancer relapse, then the timely administration of drugs targeting chemotherapy-induced senescent cells can prevent senescence escape and reduce cancer regrowth.

Although tremendous progress has been made in the treatment of breast cancer leading to improved patient outcomes, there remains a high risk for relapse that needs to be addressed. Nearly half of all breast cancer patients fail to achieve pCR following NACT. Strategies to

improve pCR and improve patient treatment outcomes rely on the augmentation of NACT with additional therapies that have limited side effects. Administering additional treatments in the neoadjuvant setting has the potential to reduce cancer regrowth. It is highly demanded to develop a strategy that timely and selectively eliminates senescent cells to prevent tumour regrowth from occurring via these senescent cells escaping from their senescent state and re-entering proliferation. Better understanding one of the mechanisms by which breast cancer may recur can facilitate the development of targeted therapeutics.

1.9 Aims and objectives

To answer my hypothesis, three aims were established. First, a pre-clinical model of chemotherapy-induced senescence will be developed. Cisplatin was chosen for the pre-clinical model of chemotherapy-induced senescence, as literature suggests that cisplatin induces cancer cells to enter senescence due to its ability to damage DNA. Acute cisplatin treatment and the subsequent removal of cisplatin treatment was chosen to mimic the chemotherapy rounds given to cancer patients. Chemotherapy regimens usually consist of chemotherapy treatment followed by periods of rest. In the off-treatment periods, patients recover from the side effects of chemotherapy. However, the ability of breast cancer cells to eventually escape from senescence also happens during the off-treatment periods.

Senescence induction will be verified in 3 ways: morphological changes, SA-β-gal staining, and changes in protein expression. Upon confirming that cisplatin does successfully induce senescence in breast cancer cells, the sensitivity of these chemotherapy-induced senescent cells to senolytics would be determined with dose-response curves and clonogenic assays.

2. Methods

2.1 Breast cancer model

The MDA-MB-231 cell line is currently one of the most widely used breast cancer cell lines for modeling advanced late-stage breast cancer. The MDA-MB-231 cell line was chosen because of its highly aggressive and invasive phenotype, which renders this cell line prone to recurrence and eventual metastasis. For highly aggressive cancers such as MDA-MB-231, it is ideal to eradicate all signs of the cancer and prevent senescence escape from resulting in relapse and the acquisition of further aggressive characteristics. MDA-MB-231 cells have also been shown to not respond to cisplatin treatment.

The PDX-derived primary cell lines conserve the molecular landscape, metastasis, chemosensitivity of the original patient tumours. None of the tumours received cisplatin treatment prior to their surgical removal and engraftment into mice. Upon further testing, GCRC1887 and GCRC1915 were both found to not shrink in response to cisplatin treatment. GCRC1863 showed only a partial response to cisplatin, indicating that although the tumour shrunk partially, there were a significant percentage of breast cancer cells that remained following cisplatin treatment (68). All three primary cell lines and MDA-MB-231 were chosen for this preclinical model because it is well-documented that these cell lines do not undergo apoptosis in response to the DNA damaging-inducing agent cisplatin.

2.2 Cell culture media

MDA-MB-231 cells were cultured in DMEM (Thermo Fisher Scientific – catalogue number 11995073) with 10% fetal bovine serum (FBS) (Thermo Fisher Scientific – catalogue number 12483020) and 50 μg / ml gentamicin (Thermo Fisher Scientific – catalogue number 15710072). The PDX-derived cell lines GCRC1863, GCRC1887, and GCRC1915 were cultured in F-media, which is 3:1 DMEM:Ham's F-12 Nutrient Mix (Thermo Fisher Scientific – catalogue number 11765062), 5% FBS, 25 ng / mL hydrocortisone (MilliporeSigma – catalogue number H0888), 5 μg / mL human recombinant insulin (Thermo Fisher Scientific – catalogue number 12585014), cholera toxin 8.4 ng / mL (MilliporeSigma – catalogue number C8052), 0.125 ng / mL epidermal growth factor (EGF) (StemCell Technologies – catalogue number 78006), 50 μg / mL gentamicin, and 10 μmol / L ROCK Inhibitor/Y-27632 Dihydrochloride (AbMole BioSciences – catalogue number M1817). All cell lines were grown at 37 °C, 5% CO2, and minimally screened for mycoplasma.

2.3 Cell culture maintenance

At approximately 70% confluency, the cells were passaged using the following protocol. The confluency was determined using a microscope at the 4X objective. The cell culture media was aspirated, the cells were washed once in 1X PBS, then Trypsin-EDTA, 0.25% (Thermo Fisher Scientific – catalogue number25200072) was added to the cells. After a 3-minute incubation at 37°C, the trypsin was inactivated by adding cell culture media. The cells were counted twice, and the count was averaged.

Generally, PDX-derived cell lines take longer to reach ~70% confluency. The MDA-MB-231 cell line was passaged twice a week. The primary breast cancer cell lines GCRC1863, GCRC1887, and GCRC1915 were passaged once a week.

2.4 Senescence induction

To develop a model in which senescence is preferentially induced instead of apoptosis, various dosages of cisplatin were given to both MDA-MB-231 cells and PDX-derived breast cancer cells. MDA-MB-231 cells and PDX-derived breast cancer cells were treated with 5 μM, 10 μM, 20 μM, and 40 μM cisplatin for an hour, then assessed for various senescence markers to examine the extent to which senescence was induced. The goal was to determine the optimal cisplatin concentration at which cells would enter a reversible senescence state. When primary cell lines were treated with cisplatin concentrations of 20 μM or 40 μM, there were little to no cells resuming their original non-senescent morphology even 2 weeks post-treatment, suggesting that the cells may require longer periods of time to re-enter proliferation when treated with high doses of cisplatin. These results suggest that in PDX-derived breast cancer cells, 10 μM cisplatin treatment for 1-hour is the optimal dosage that causes cells to both enter senescence by day 3, but also re-proliferate by day 11. Since MDA-MB-231 cells divide more aggressively, the cisplatin concentration necessary for these cells to enter senescence was higher. The optimal cisplatin concentration was determined to be 40 μM for MDA-MB-231 cells, and 10 μM for all the PDX-derived breast cancer cells.

2.5 SA-β-gal staining

Senescence induction was verified through SA-β-gal staining. The Senescence β-Galactosidase Staining Kit (Cell Signaling Technology – catalogue number 9860) was used to visualize SA-β-gal activity in cells, the most widely used biomarker for senescent cells. All solutions are prepared just prior to use. An aliquot of the 10X Fixative Solution was diluted to 1X with distilled water. The 10X Staining Solution was redissolved in a warm water bath at 37°C for 15 minutes before an aliquot was diluted to 1X with distilled water. In a light resistant

container, 20 mg of X-Gal was dissolved in 1 mL of dimethylformamide to produce a 20 mg/mL stock solution of X-Gal. The β-Galactosidase Staining Solution that is added to the cells is a mix of the following 4 reagents in the ratio indicated: 930 μL of 1X Staining Solution, 10 μL of 100X Solution A, 10 μL of 100X Solution B, and 50 μL of the X-gal stock solution. The final pH of the β-Galactosidase Staining Solution must be at ~6.0 to avoid any false positives or false negatives. The pH of the β-Galactosidase Staining Solution was adjusted to be between the range of 5.9 to 6.1 using 1N HCl. The pH was confirmed by pH-indicator strips (EMD Millipore – catalogue number 109533).

Upon preparing all the solutions, the cell culture media was aspirated, the cells were washed once with 1X PBS, and then fixed with 1X Fixative Solution. After 15 minutes, the cells were washed twice with 1X PBS, and then stained with the β-Galactosidase Staining Solution. The plates were incubated for 14 to 16 hours in a dry incubator at 37°C with no CO2. Only incubators without CO2 were used because CO2 can change the solution's pH, consequently affecting the amount of SA-β-gal staining. The plates were sealed tightly with parafilm to prevent any evaporation during the incubation period. Evaporation can lead to the formation of crystals, which can interfere with the visualization of SA-β-gal activity. After 14 to 16 hours, the plates were imaged using the EVOS M7000 microscope.

The total number of senescent cells was counted using ImageJ. The Mean Gray Area value (Analyze → Set Measurements) determined by ImageJ was used to establish the threshold for a cell to be considered blue. Using the oval selection tool, each cell was outlined, and the Mean Gray Area was measured (Analyze → Measure). The percentage of senescent cells in the total cell population was calculated in Excel and graphed using Prism.

2.6 Western blot

Western blots were performed as another method to confirm cellular senescence. Cells harvested on day 4 after 1-hour cisplatin treatment were seeded at a density of 100,000 cells / well in a 6-well plate. This seeding density allowed the wells to be ~50% confluent by day 4. Cells harvested on day 7 were seeded at half the density of 50,000 cells / well to prevent over-confluency. The following procedures were performed on ice to reduce protease activity and prevent protein denaturation (70). Cells were washed once with ice cold 1X PBS. Proteins were collected by incubation with the RIPA lysis buffer for 30 minutes at 4°C, lysing the cells. The RIPA lysis buffer consisted of 0.15 M NaCl, 0.005 M EDTA pH 8.0, 5% 1 M Tris-Cl pH 8.0, 1% NP-40 (IGEPAL CA630), 0.1% SDS, 0.05% sodium deoxycholate, 5 mM NaF, 0.01 M NaPP, and 20 mM β-glycerophosphate. Prior to adding the RIPA lysis buffer to cells, 0.1% leupeptin, 0.1% aprotinin, 0.5% Na3VO4, 1% AEBSF were added. Then, the samples were centrifuged at 15,000 RPM for 15 minutes. The supernatant was collected in new tubes on ice, and the pellet was disregarded. The protein lysates were stored at -20°C.

Protein concentrations were determined following detergent solubilization with a colorimetric assay, the detergent compatible (DC) protein assay (Bio-Rad – catalogue number 5000116). Following the microplate assay protocol provided by Bio-Rad, 8 different protein standards were prepared (0 mg/mL, 0.2 mg/mL, 0.4 mg/mL, 0.6 mg/mL, 0.8 mg/mL, 1.0 mg/mL, 1.2 mg/mL, and 1.4mg/mL protein). A standard curve was prepared every time the DC protein assay was performed. The protein lysates were diluted 1:10 with distilled water before their concentrations were measured. Using a 96-well plate, 5 uL of the protein standards and diluted protein samples were added to the wells in triplicates. Then, a working reagent A' was prepared by adding 20 μL of reagent S to every 1 mL of reagent A required. Into each well, 25 μL of

reagent A' and 200 µL of reagent B were added. The plate was gently agitated to mix the reagents. After 15 minutes incubation, the plate's absorbance can be measured at 750 nm.

The 10X Running Buffer consisted of 30.3 g Tris base, 144.0 g glycine, and 10.0 g SDS in 1 L of distilled water. No pH adjustment was required. The 10X Running Buffer was stored at room temperature and was diluted to 1X prior to each gel electrophoresis run. 6X SB consisted of 15 mL of 300 mM Tris-HCl pH 6.8, 15 mL of 30% glycerol, 5.0 g of 10% SDS, 1% bromophenol blue, in 50 mL of distilled water. 2-mercaptoethanol was added just prior to each use of SB. The volume of protein lysate required for 30 µg was added to a microtube, and 7.5 µL of 6X SB + 10% 2-mercaptoethanol (BioShop – catalogue number MER002) were added. The total volume was brought to 30 µL by adding distilled water. The mixture was heated at 95°C for 5 minutes and then given a quick spin in a centrifuge. 28 µL of the mixture was loaded into the 4–20% Precast Gels (Bio-Rad – catalogue number 4568094) used for protein separation. In each gel, 5 µL of Protein Dual Color Standards (Bio-Rad – catalogue number 1610374) were loaded to estimate the molecular weight of any proteins of interest. The gel electrophoresis was run at a constant voltage of 200 volts for 30 to 45 minutes. The gel electrophoresis was stopped as soon as the blue band disappeared from the bottom of the gel.

The 10X Transfer Buffer consisted of 30.3 g Tris base and 144.0 g glycine dissolved in 1 L of distilled water. No pH adjustments were made to the buffer. The 10X Transfer Buffer was diluted to 1X prior to each use, and 200 mL of methanol were added to the 1X Transfer Buffer. The membrane was activated by placing it in methanol for 3 seconds before placing it in 1X Transfer Buffer. After assembling the transfer sandwich of sponge, 2 filter papers, gel, membrane, 2 filter papers, sponge, roll a test tube gently over the transfer sandwich to ensure there are no air bubbles between the gel and the membrane. All components of the transfer sandwich were soaked in 1X Transfer Buffer to equilibrate the transfer sandwich. The transfer is

performed at a constant current of 0.30 ampere for 1 hour in a 4°C cold room. An ice pack was put in the apparatus to prevent overheating during the transfer process.

The membranes were incubated at room temperature with 5% milk for 1 hour to saturate any non-specific protein binding sites on the membranes. This step reduces background and enhances sensitivity for the proteins of interest. The membranes were then incubated at 4°C with a primary antibody for 12-16 hours. The lamin B1 antibody (Abcam – catalogue number ab16048) was diluted 1:1000 in 5% milk. The p21 antibody (Cell Signaling Technology – catalogue number 2947) was diluted 1:1000 in 5% BSA. Vinculin was the loading control used to show that all samples were loaded equally. The antibody for vinculin was diluted 1:10,000 in 5% milk. Both the 5% milk and the 5% BSA solutions were dissolved in TBST. The 10X TBS consisted of 24.2 g Tris base and 80.0 g NaCl dissolved in 1 L of distilled water. The pH was adjusted to be at 7.6 using 1N HCl. TBST solution was made from the addition of 0.1% Tween (Sigma-Aldrich – catalogue number P1379) to 1X TBS.

After incubation with the primary antibody overnight at 4°C, the membranes were washed in TBST three times, for 5 minutes each time. The membranes were then incubated at room temperature with a secondary antibody for 1 hour. Both mouse and rabbit secondary antibodies were diluted 1:10,000 in 5% milk. After incubation with the secondary antibody, the membranes were washed in TBST three times, for 5 minutes each time. The membranes were then washed a final time in TBS before being imaged at the ChemiDoc Imaging System.

The West Femto Peroxide Buffer and Luminol (Thermo Fisher Scientific – catalogue number 34095) were mixed in a 1:1 ratio and 500 μL of the mixture was applied to each of the membranes right before the membranes were imaged. Protein bands were detected with 0.1 seconds of chemiluminescence. The protein ladder was captured using 0.1 seconds of

colorimetric detection. The images are then merged to verify the molecular weight of the protein bands.

2.7 Dose-response curves

Dose-response experiments were performed with navitoclax. Breast cancer cells were induced to senesce by 1-hour treatment with the DNA-damaging agent, cisplatin. The cisplatin treatment was then washed off and the cells were given F-media. Senescent cells were trypsinized on day 3 following cisplatin treatment and seeded in 96-well plates along with proliferating untreated cells. The most optimal cell seeding density was first determined by seeding each of the primary cell lines at various densities and verifying that the control groups not given navitoclax reach ~70% confluency after 6 days. Starting day 4 after cisplatin treatment, the cells were cultured in F-media with various navitoclax concentrations for 6 more days. The following navitoclax concentrations were used: 20 μM, 10 μM, 5 μM, 2.5 μM, 1.25 μM, 0.625 μM, 0.3125 μM, 0.156 μM, and 0 μM. All media solutions were prepared with a serial dilution from a 10 mM stock solution of navitoclax.

After 6 days, cell viability was determined using the CellTiter-Blue Cell Viability Assay (Promega Corporation – catalogue number G8081). The assay contains a redox dye, resazurin, which is converted to a fluorescent product, resorufin, by cells that are metabolically active. The presence of metabolic capacity indicates that the cell is viable. Non-viable cells in the culture would not generate a fluorescent signal, as they are unable to reduce resazurin into resorufin. Thus, the fluorescent signal is proportional to the number of viable cells in culture.

At the experiment's endpoint of 6 days, the CellTiter-Blue Reagent was diluted 1:1 in the cell culture media, and 20 μL of the diluted Reagent was added into each of the wells in a 96-well plate. The CellTiter-Blue Reagent was protected from light as much as possible during the

process, as prolonged exposure of the CellTiter-Blue Reagent to light will increase background levels of fluorescence. The plates were incubated at 37°C for 2 hours to allow any viable cells to convert resazurin into resorufin. Afterwards, the plate's fluorescence was measured using 544nm for excitation and 590nm for emission. The fluorescent signals were measured in triplicates and averaged using Excel.

2.8 Clonogenic assays

The most optimal cell seeding density was determined by seeding each of the cell lines at various densities and checking the confluency of the wells every 3 days until the experiment's endpoint of 2 weeks. In 24-well plates, cells were seeded at densities of 1000, 2500, 5000, 7500, and 10,000 cells per well. After determining the most optimal seeding density, control cells were plated at densities of 2500 cells per well while senescent cells were plated at 10,000 cells per well in the 24-well plates. Control cells were plated at a relatively lower density than senescent cells to prevent over-confluency prior to the experiment's endpoint.

The cells were washed once with 1X PBS and then incubated with 0.5% crystal violet staining solution (Sigma-Aldrich – catalogue number HT90132) for 30 minutes on a shaker. After 30 minutes, the crystal violet staining solution was washed off with water. Crystal violet binds to proteins and DNA of adhered cells. Since adherent cells detach from cell culture plates during cell death, cells that undergo apoptosis lose their adherence and are subsequently not stained by crystal violet, reducing the total amount of crystal violet staining (71).

For the MDA-MB-231 cell line, the cells were stained with crystal violet solution at an endpoint of 10 days. The breast cancer cell lines derived from PDXs were stained with crystal violet solution at an endpoint of 18 days, giving the colonies more time to proliferate due to their slower growth rates. The amount of crystal violet staining was quantified by dissolving the cells

in 10% acetic acid (BioShop – catalogue number ACE222). After 20 minutes, the samples were diluted 1:4 in water before measuring the samples' absorbance at 590 nm. The more colonies adhered to the cell culture plate, the higher the absorbance at 590 nm.

2.9 Statistical analysis

Statistical significance was determined using Welch's t-test in Prism. Welch's t-test, also known as the unequal variances t-test, is a modification of Student's t-test that evaluates if the mean values of two samples are significantly different (72). When the two groups have equal sample sizes and variances, Welch's t-test would give the same result as Student's t-test. However, when sample sizes and variances are unequal, Student's t-test becomes rather unreliable, and Welch's t-test tends to perform better (72). In our statistical analyses, outliers were defined as values more than 2 standard deviations away from the mean and were excluded from the graphs.

3. Results

The three different ways by which senescence induction was verified are presented below. Firstly, the enlarged and flattened cellular morphology was evident under the microscope several days after cisplatin treatment. Secondly, the increase in SA-β-gal staining confirms that breast cancer cells enter senescence as a result of acute cisplatin treatment. Lastly, changes in protein expression levels indicate that senescence induction occurred following cisplatin treatment. Specifically, levels of p21 and Lamin B1 were measured.

3.1 Morphological changes

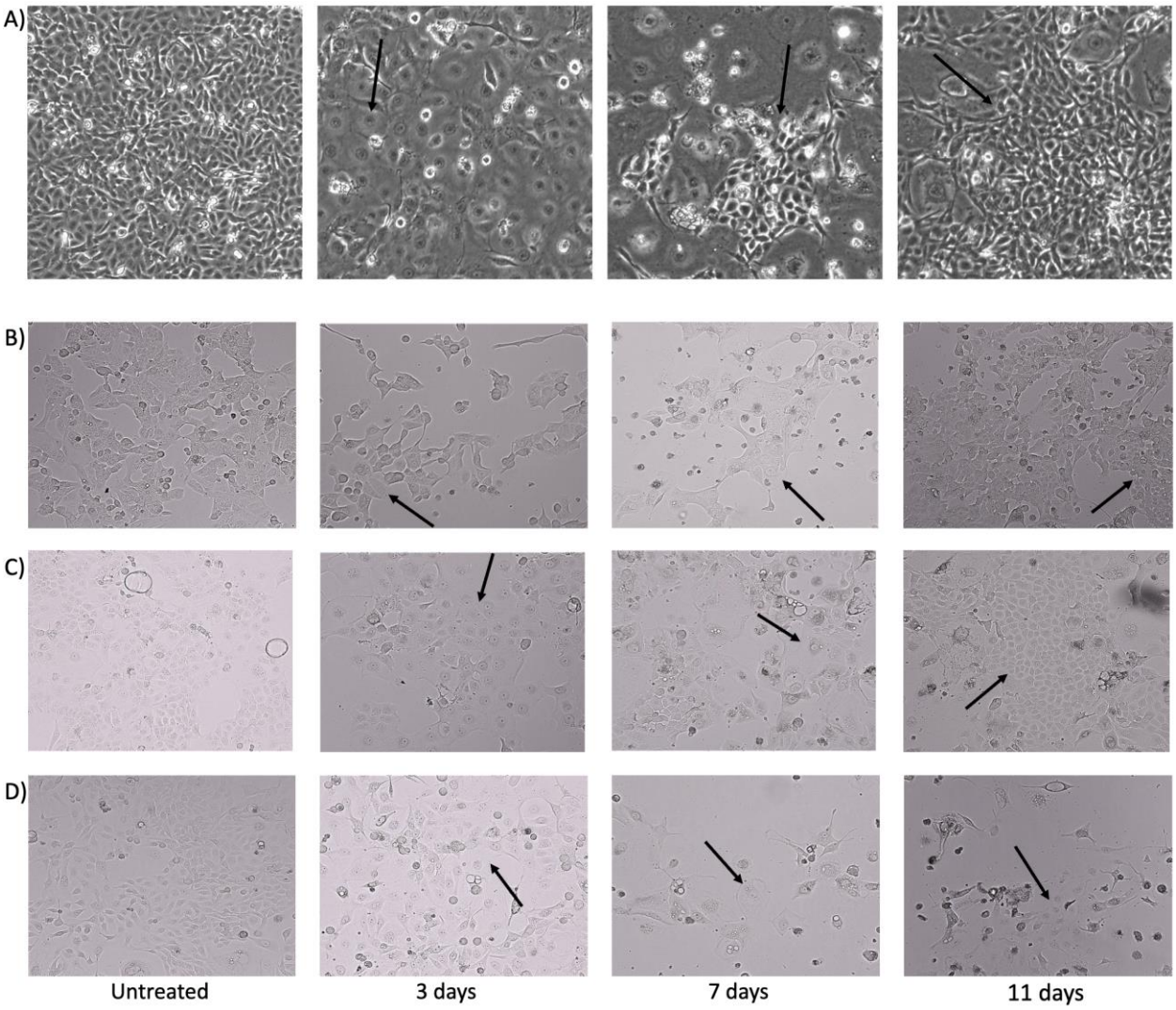

Figure 7. Cellular morphology of breast cancer cells following senescence induction with cisplatin. (A) Morphology of MDA-MB-231 cells 3 days, 7 days, and 11 days after treatment with 40 μM cisplatin for 1 hour. (B) Morphology of GCRC1863 cells 3 days, 7 days, and 11 days after treatment with 10 μM cisplatin for 1 hour. (C) Morphology of GCRC1887 cells 3 days, 7 days, and 11 days after treatment with 10 μM cisplatin for 1 hour. (D) Morphology of GCRC1915 cells 3 days, 7 days, and 11 days after treatment with 10 μM cisplatin for 1 hour. Black arrows point towards any notable changes in cellular morphology.

One major hallmark of senescent cells is their enlarged and flattened cellular morphology. Senescent cells undergo drastic morphological changes, increasing in both cell and mitochondrial size (73). The evident change in cellular morphology is one of the means by which senescence induction was verified. Cells treated with saline instead of cisplatin did not undergo any morphological changes in the following weeks. MDA-MB-231 cells treated with 40 μM of cisplatin increased in average cell size by day 3 after cisplatin treatment. By day 7 after cisplatin treatment, a select population of MDA-MB-231 cells begin to resume the original morphology (Fig. 7). For the PDX-derived breast cancer cells GCRC1863, GCRC1887, and GCRC1915, a select population of cells begin to display this characteristic change by day 3, but the cells' enlargement was more evident a few days later. GCRC1863, GCRC1887, and GCRC1915 were more visibly enlarged by day 7 after cisplatin-treatment. The slower change in morphology may be explained by the slower cell growth rate observed in primary cancer cells compared to the more highly aggressive and invasive MDA-MB-231. By 11 days after acute cisplatin exposure, colonies resembling the original pre-treatment morphology begin to re-appear in all the PDX-derived cell lines (Fig. 7). This observation is consistent with the hypothesis that senescence escape occurs in the off-treatment periods between chemotherapy rounds, resulting in the cancer's regrowth.

3.2 Increase in senescence-associated β-galactosidase

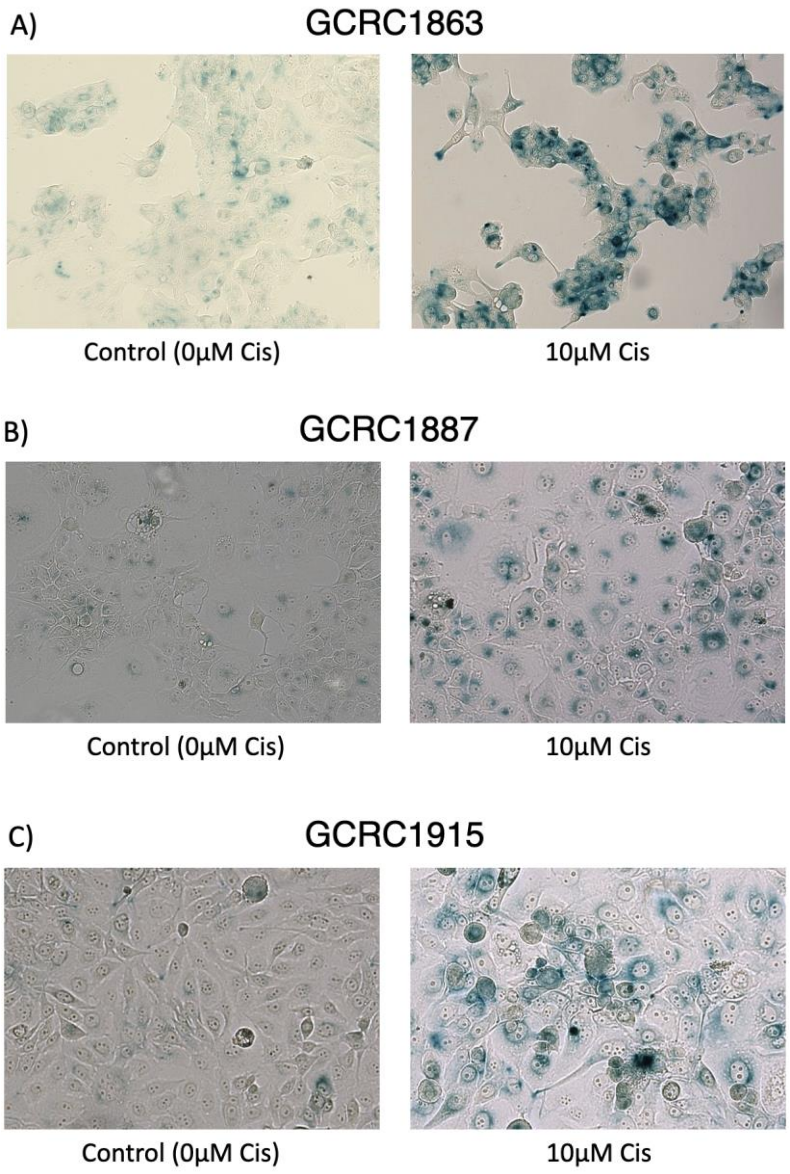

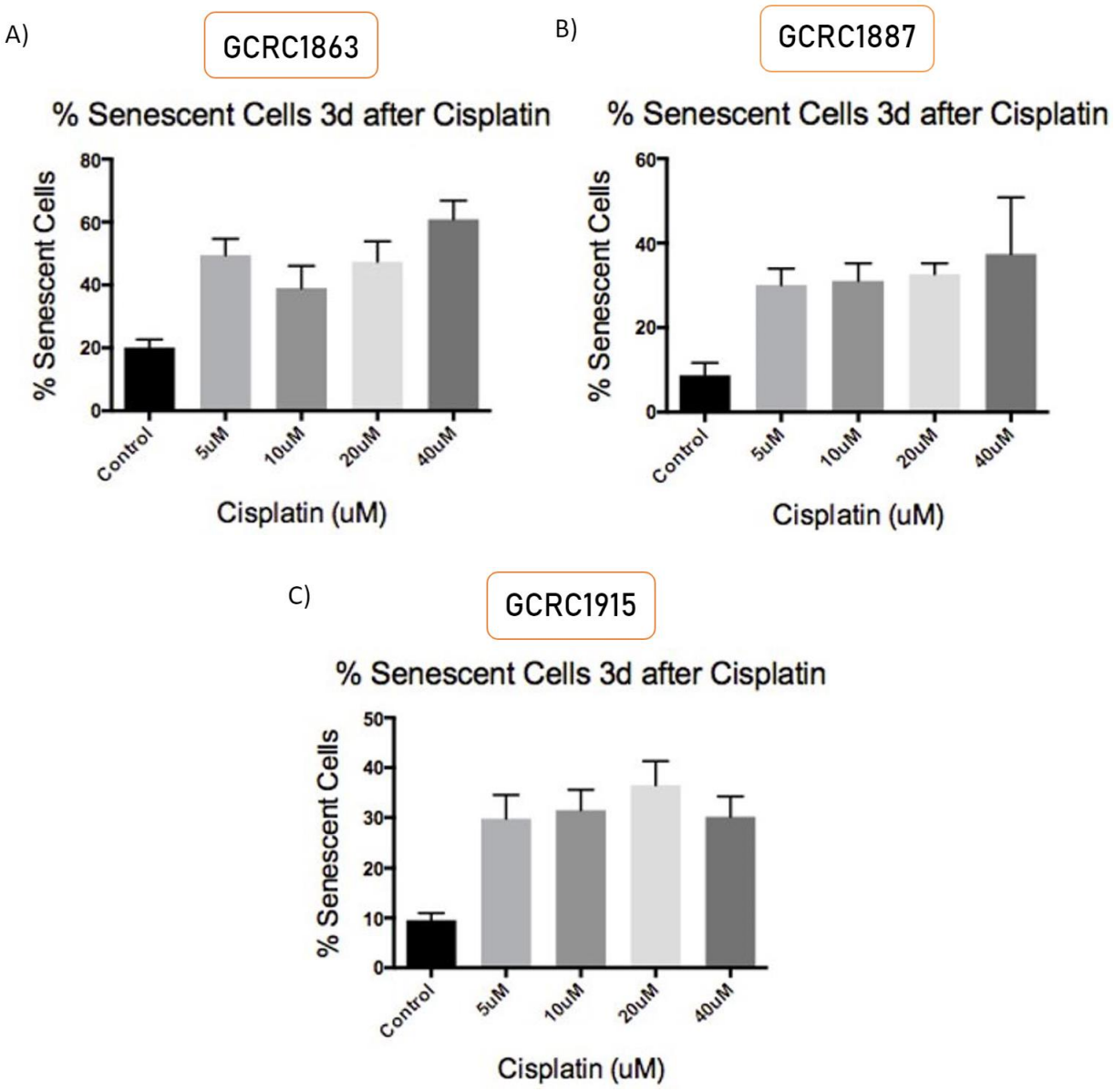

Figure 8. **Increase in the percentage of senescent cells 3 days after 1-hour cisplatin treatment, as determined by SA-β-gal staining.** (A) Images of GCRC1863 breast cancer cells after SA-β-gal staining incubation of 14 to 16 hours. Percentage of blue cells were counted using ImageJ. (B) Images of GCRC1887 breast cancer cells after SA-β-gal staining incubation of 14 to 16 hours. Percentage of blue cells were counted using ImageJ. (C) Images of GCRC1915 breast cancer cells after SA-β-gal staining incubation of 14 to 16 hours. Percentage of blue cells were counted using ImageJ. Cells were imaged using the EVOS M7000 microscope.

In addition to an increase in average cell size, senescent cells also have elevated levels of a lysosomal enzyme, SA-β-gal. SA-β-gal is the gold standard marker for senescence in vitro and has been shown to be a very robust indicator (74, 75). SA-β-gal staining can differentiate between cellular senescence and quiescence, although both cell types are growth-arrested. Thereby, only senescent cells would appear to be stained blue (Fig. 8). An increase in SA-β-gal staining is the second method by which senescence induction was verified in our preclinical model. Breast cancer cells treated with saline had a significantly lower percentage of blue cells when stained with SA-β-gal compared to cells treated with any concentration of cisplatin (Fig. 8). This would be the baseline level of senescent cells in culture, which was 10% for GCRC1887 and GCRC1915 cell lines, and 20% for GCRC1863. The use of a specific Mean Gray Area value as a threshold for senescent cells on ImageJ accounted for the different background tints seen among the different experimental conditions. Following cisplatin treatment for an hour, there was a significant increase in the number of senescent cells, irrespective of whether cells were treated with 5 μM, 10 μM, 20 μM, or 40 μM of cisplatin (Fig. 8). These results suggest that even lower dosages of cisplatin exposure for an hour can induce these primary cells to enter a state of senescence by day 3 post-cisplatin. Higher cisplatin concentrations did not significantly affect the percentage of primary cells induced into senescence.

3.3 Protein expression in senescent cells

The expression levels of several proteins are known to be different in senescent cells. The levels of p21 and Lamin B1 were normalized to the levels of the loading control, vinculin.

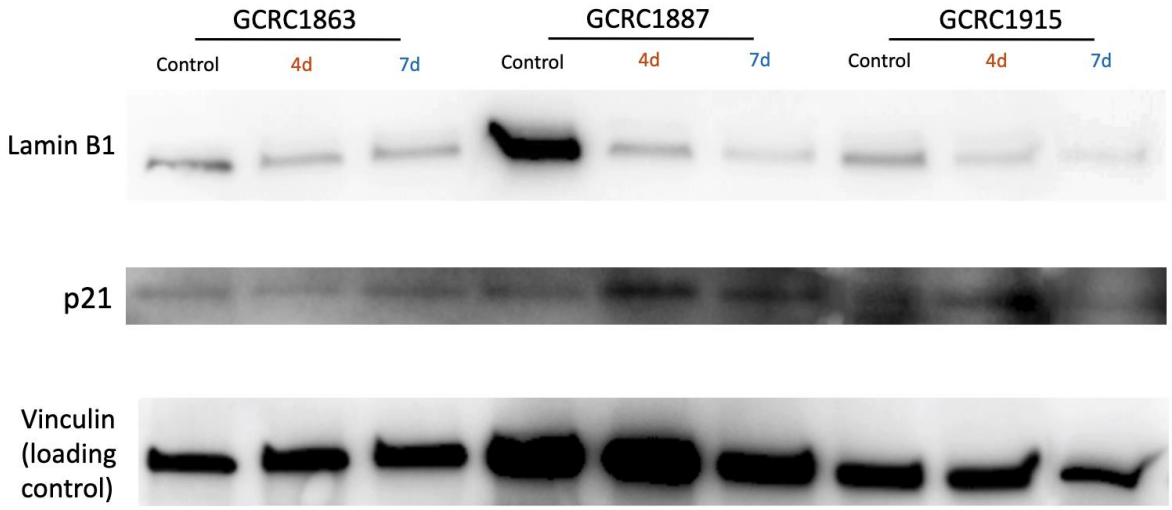

Figure 9. Changes in p21 and Lamin B1 levels after senescence induction with cisplatin. Protein expression levels were determined using a western blot. The molecular weight of Lamin B1 is 66 kDa. The molecular weight of vinculin is 124 kDa. The molecular weight of p21 is 21 kDa. All protein bands were detected at the expected molecular weight.

Extensive literature suggest that decreased Lamin B1 levels can serve as a biomarker of senescence in vitro (73). 4 days after acute cisplatin exposure, all primary cell lines (GCRC1863, GCRC1887, GCRC1915) have significantly decreased amounts of Lamin B1 (Fig. 9). GCRC1863 showed a ~25% decrease in Lamin B1 levels (n=2); GCRC1887 showed a ~40% decrease (n=2); GCRC1915 showed a ~55% decrease (n=2). 7 days after acute cisplatin exposure, the primary cell lines had further decreased levels of Lamin B1. Specifically, GCRC1863 showed a ~60% decrease in Lamin B1 at day 7 (n=2), which was significantly greater than the ~25% decrease seen at day 4. Similarly, GCRC1887 showed an ~85% decrease in Lamin B1 at day 7 (n=2), a significantly larger decrease than the ~40% seen at day 4. Lastly, GCRC1915 had an ~80% decrease at day 7 (n=1).

To confirm senescence induction after DNA damage, p21 levels were also measured after acute cisplatin exposure. Upregulation of p21 has been shown to lead to cell cycle arrest in senescent cells (76). p21 inhibits CDK complexes that mediate cell cycle progression (77). For the GCRC1863 cell line, there is a more than 3 times increase in p21 levels at day 7 (n=2). p21 levels were only increased at day 4 for both GCRC1887 and GCRC1915, but not at day 7. Preliminary results of n=1 from the GCRC1915 cell line show that p21 levels in fact decrease to levels lower than base line on day 7 after chemotherapy-induced senescence. This observation can be explained by the fact that the induction of p21 in senescent cells is only transient; protein levels of p21 decrease after cell cycle arrest is established (76).

3.5 Navitoclax dose-response curves

A dose-response curve was generated to determine the sensitivity of chemotherapy-induced senescent breast cancer cells to the senolytic drug, navitoclax.

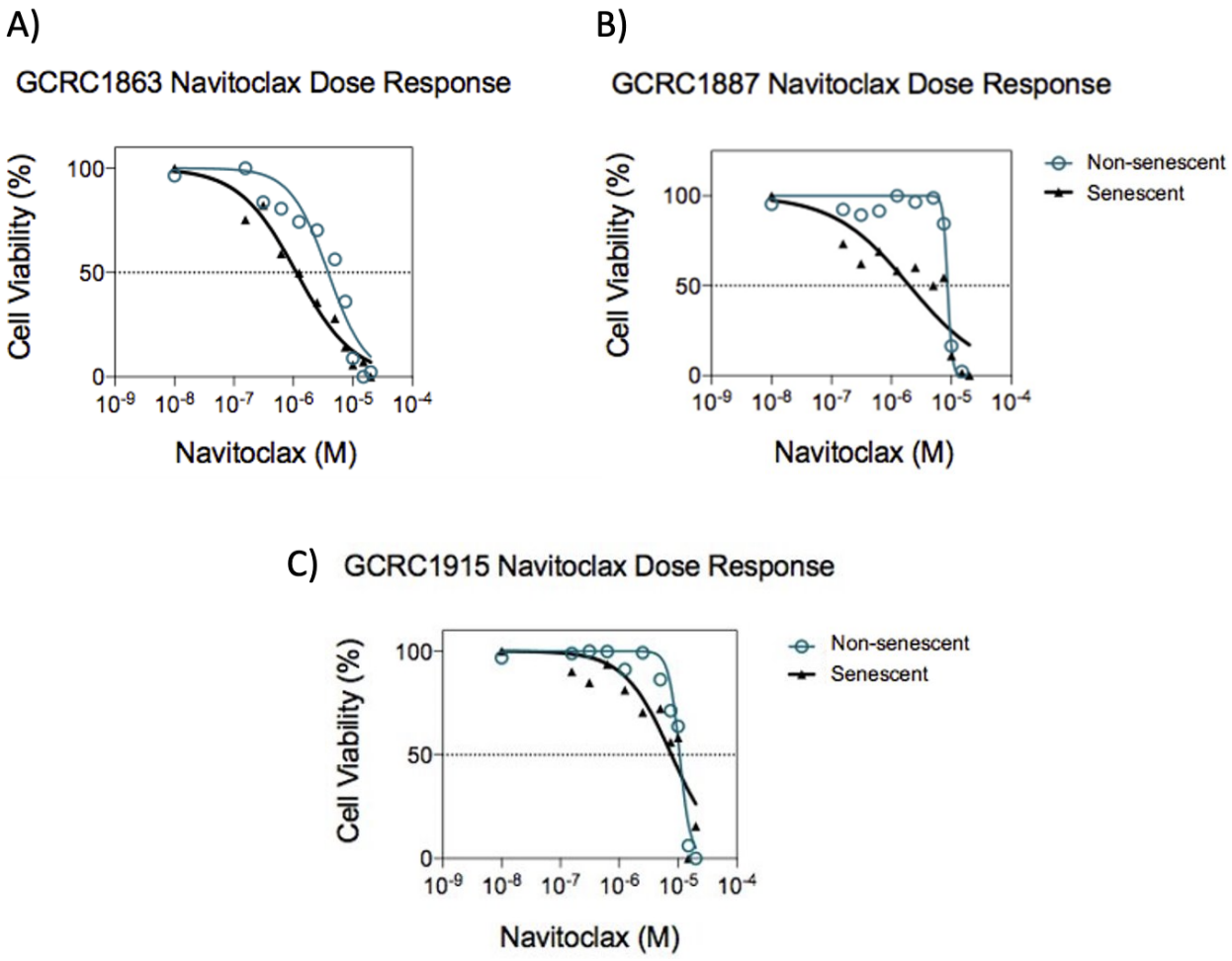

Figure 10. Sensitivity of senescent and non-senescent breast cancer cells to the senolytic navitoclax. PDX-derived breast cancer cells were treated with nine different doses of navitoclax to generate a dose-response curve. (A) Dose-response curve generated for GCRC1863 cells (n=3). (B) Dose-response curve generated for GCRC1887 cells (n=3). (C) Dose-response curve generated for GCRC1915 cells (n=3). Cell viability data was averaged across triplicates. Cell viability for both senescent and non-senescent cells were normalized to the cell population that was not treated with navitoclax. The EC50 value is the navitoclax concentration at which the relative number of viable cells at the experiment's endpoint is 50%.

The half maximal effective concentration, EC50, is a direct measure of the potency of a drug (78). EC50 is defined as the drug concentration at which half of the maximum possible

response is induced, which in this experiment is the dose at which the drug navitoclax eliminates 50% of breast cancer cells. For each cell line, cells that were induced into senescence were compared to control cells in terms of their sensitivity to navitoclax. As navitoclax selectively eliminates senescent cells, chemotherapy-induced senescent cells were expected to have a lower EC50 than control cells, which means that a lower navitoclax dosage is required to eliminate 50% of the cell population. For all 3 PDX-derived cell lines (GCRC1863, GCRC1887, GCRC1915), there was a leftward shift in the dose response observed for the senescent cell group (Fig. 10). There was a more significant leftward shift observed for the GCRC1863 and GCRC1887 cell lines (Fig. 10A, Fig. 10B). This is consistent with the hypothesis that chemotherapy-induced senescent cells would be more responsive to senolytics.

3.6 Clonogenic assays

Clonogenic assays were performed to measure the extent to which breast cancer cells proliferated in the weeks following treatment with a senolytic drug. The growth of non-senescent cells were compared to the senescent cell group.

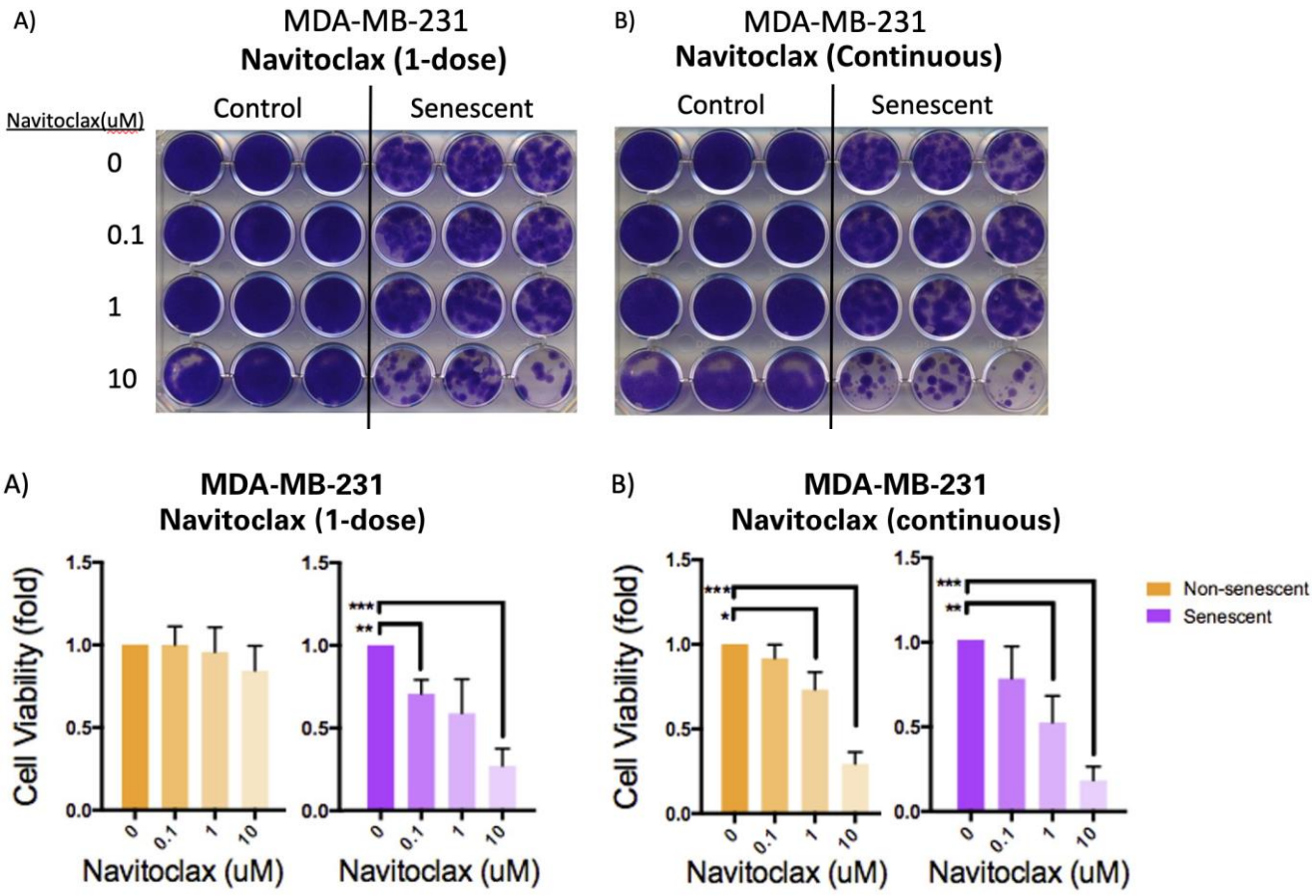

Figure 11. Clonogenic assays with the senolytic navitoclax administered once or continuously to MDA-MB-231 cells. (A) MDA-MB-231 cells were treated with navitoclax on day 4 post-cisplatin treatment, and navitoclax was removed from the culture media after 3 days. (B) MDA-MB-231 cells were treated continuously with the indicated dosage of navitoclax from day 4 post-cisplatin treatment until the experiment's endpoint. The plates were stained with 0.5% crystal violet staining solution. One asterisk represents $0.01 < \text{p-value} \leq 0.05$. Two asterisks represent $0.001 < \text{p-value} \leq 0.01$. Three asterisks represent $0.01 < \text{p-value} \leq 0.001$.

The Welch's t-test was used to identify any statistical differences in the quantity of adherent cells at the experiment's endpoint. The chemotherapy-induced senescent cells were selectively eliminated by one-time administration of the additional senolytic drug, navitoclax (Fig. 11A). When the additional senolytic drug was given at high doses and continuously until the experiment's endpoint, the drug was no longer specifically eliminating senescent cells. When higher dosages of navitoclax (1 μM, 10 μM) were administered continuously, both control cells and senescent cells were eliminated by navitoclax (Fig. 11B). Thus, when the clonogenic assay was performed in primary cell lines, the senolytic was only administered one-time and not continuously.

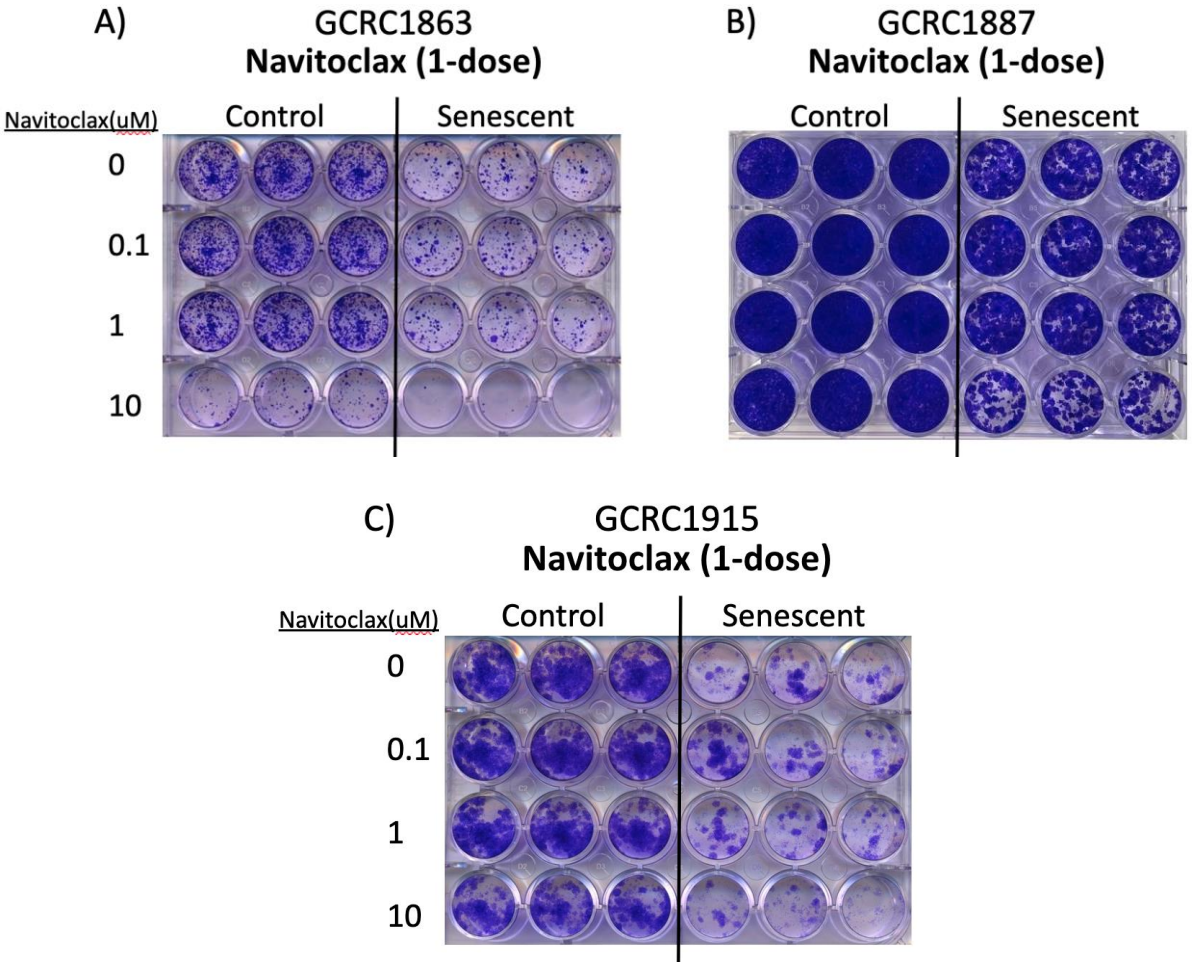
A)
GCRC1863
Navitoclax (1-dose)
Navitoclax(uM)
Control
Senescent
0
0.1
1
10
B)
GCRC1887
Navitoclax (1-dose)
Control
Senescent
C)
GCRC1915
Navitoclax (1-dose)
Navitoclax(uM)
Control
Senescent
0
0.1
1
10

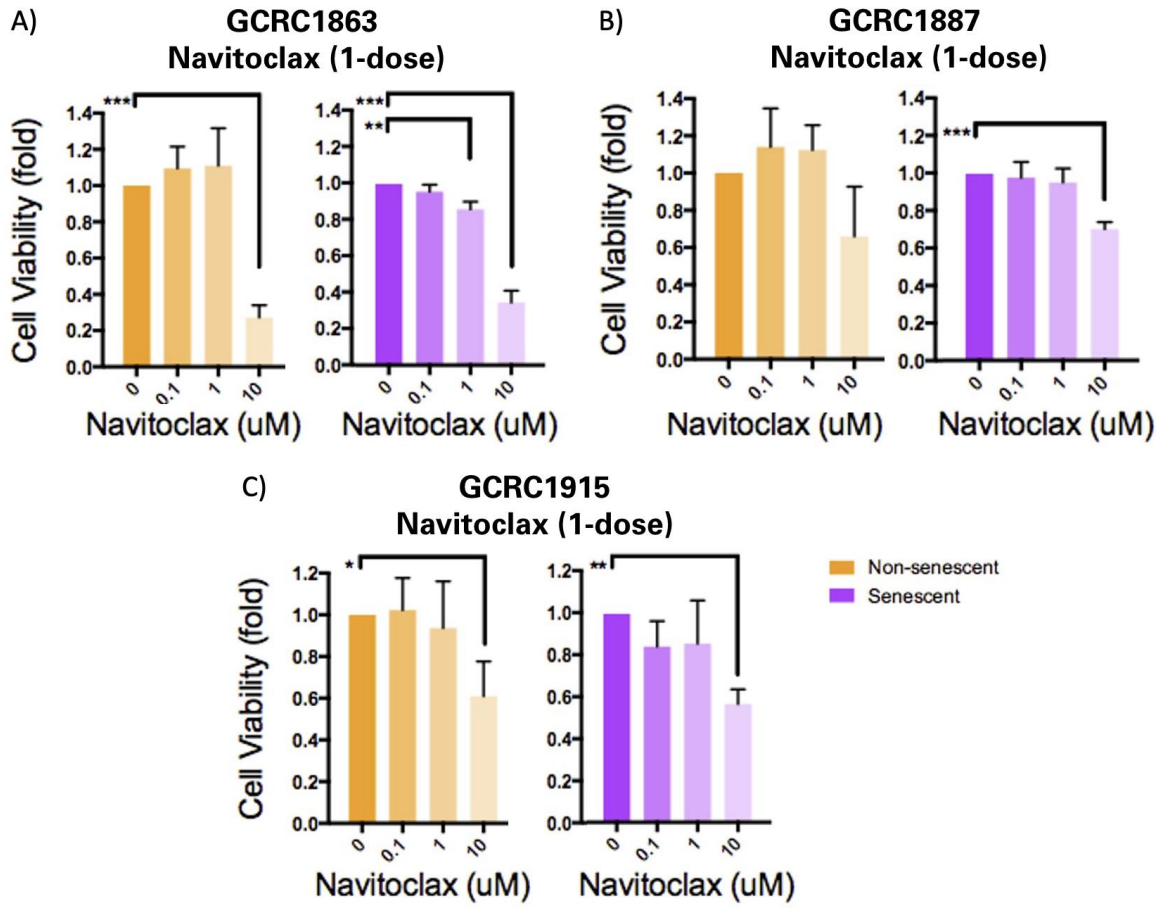

Figure 12. Clonogenic assays with the senolytic navitoclax in PDX-derived breast cancer cell lines GCRC1863, GCRC1887, and GCRC1915. (A, B, C) GCRC1863, GCRC1887, or GCRC1915 cells were treated with navitoclax on day 4 post-cisplatin treatment, and navitoclax was removed from the cell culture media after 3 days. The plates were stained with 0.5% crystal violet staining solution. One asterisk represents $0.01 < \text{p-value} \leq 0.05$. Two asterisks represent $0.001 < \text{p-value} \leq 0.01$. Three asterisks represent $0.01 < \text{p-value} \leq 0.001$.

For GCRC1863 and GCRC1915, high doses of navitoclax (10 μM) eliminated both non-senescent and senescent breast cancer cells (Fig. 12A, Fig. 12C). For the GCRC1863 cell line, a significant difference was observed between non-senescent and chemotherapy-induced senescent cells in response to 1 μM of navitoclax treatment (Fig. 12A). The senescent cell population was more selectively eliminated by 1 μM navitoclax. For the GCRC1887 cell line, senescent cells

were significantly more sensitive (p-value < 0.001) to the addition of 10 μM navitoclax to the cell culture media (Fig. 12B). There was a ~30% decrease in cell viability in the senescent cell group, but no significant decrease in cell viability for the control group. For the GCRC1915 cell line, senescent cells showed a more statistically significant decrease in cell viability in response to 10 μM of navitoclax (p-value < 0.01). Although the dosage at which the senescent cells become more susceptible to killing by navitoclax differs between the 3 primary cell lines, the results suggest that there is a concentration at which senescent cells are more selectively eliminated by navitoclax than non-senescent cells.

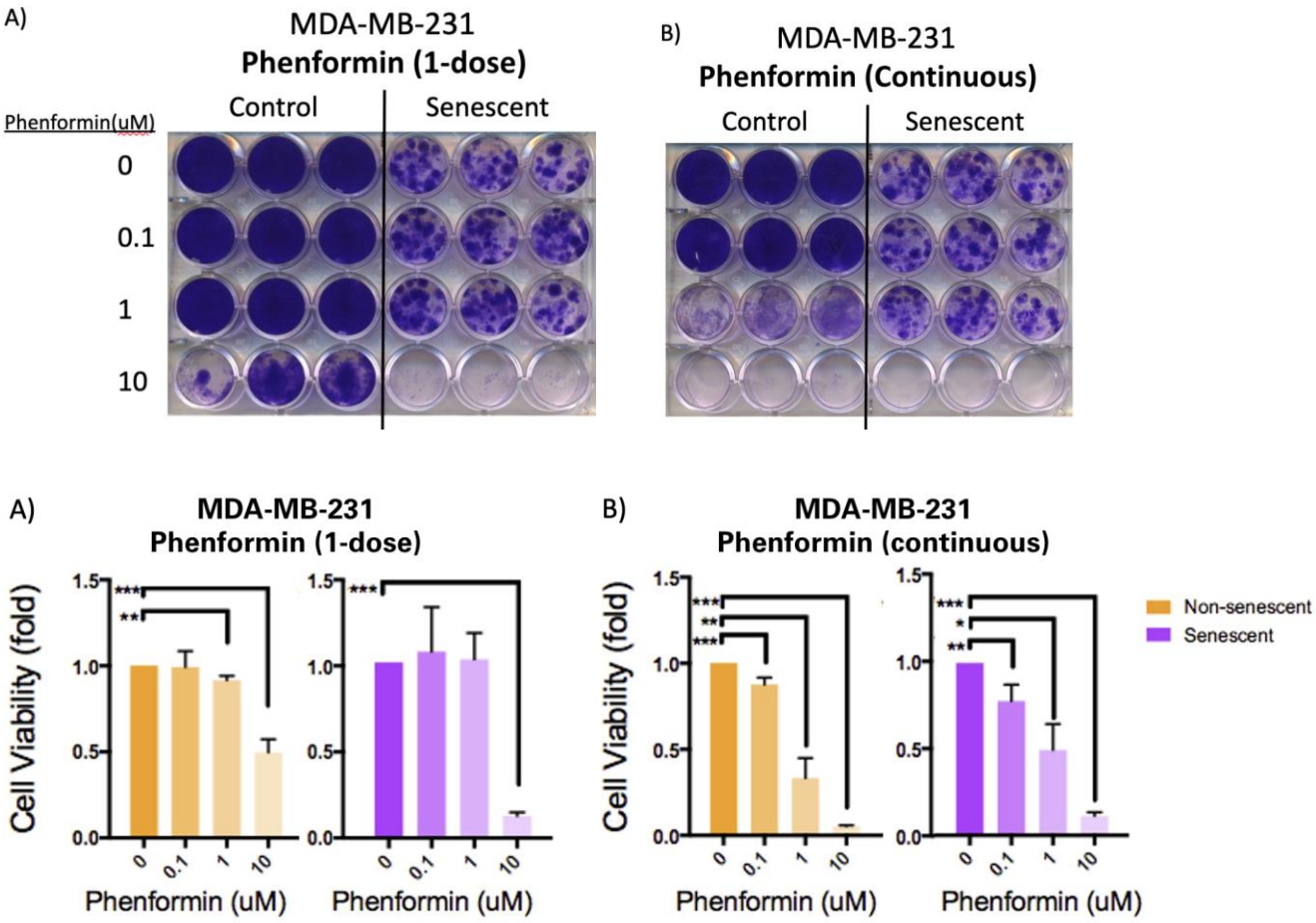

Figure 13. Clonogenic assays with the drug phenformin administered once or continuously to MDA-MB-231 cells. (A) MDA-MB-231 cells were treated with phenformin on day 4 post-cisplatin treatment, and phenformin was removed from the media after 3 days. (B) MDA-MB-231 cells were treated continuously with the indicated dosage of phenformin from day 4 post-cisplatin treatment until the experiment's endpoint. The plates were stained with 0.5% crystal violet staining solution. One asterisk represents $0.01 < \text{p-value} \leq 0.05$. Two asterisks represent $0.001 < \text{p-value} \leq 0.01$. Three asterisks represent $0.01 < \text{p-value} \leq 0.001$.

Cells treated with low doses of phenformin proliferated at similar rates to control cells that were given no additional phenformin treatment (Fig. 13A). When phenformin was added continuously to the cell culture media until the experiment's endpoint, the drug was no longer

specifically targeting senescent cells (Fig. 13B). Even low doses of phenformin (0.1 μM) were toxic to all cells when administered continuously.

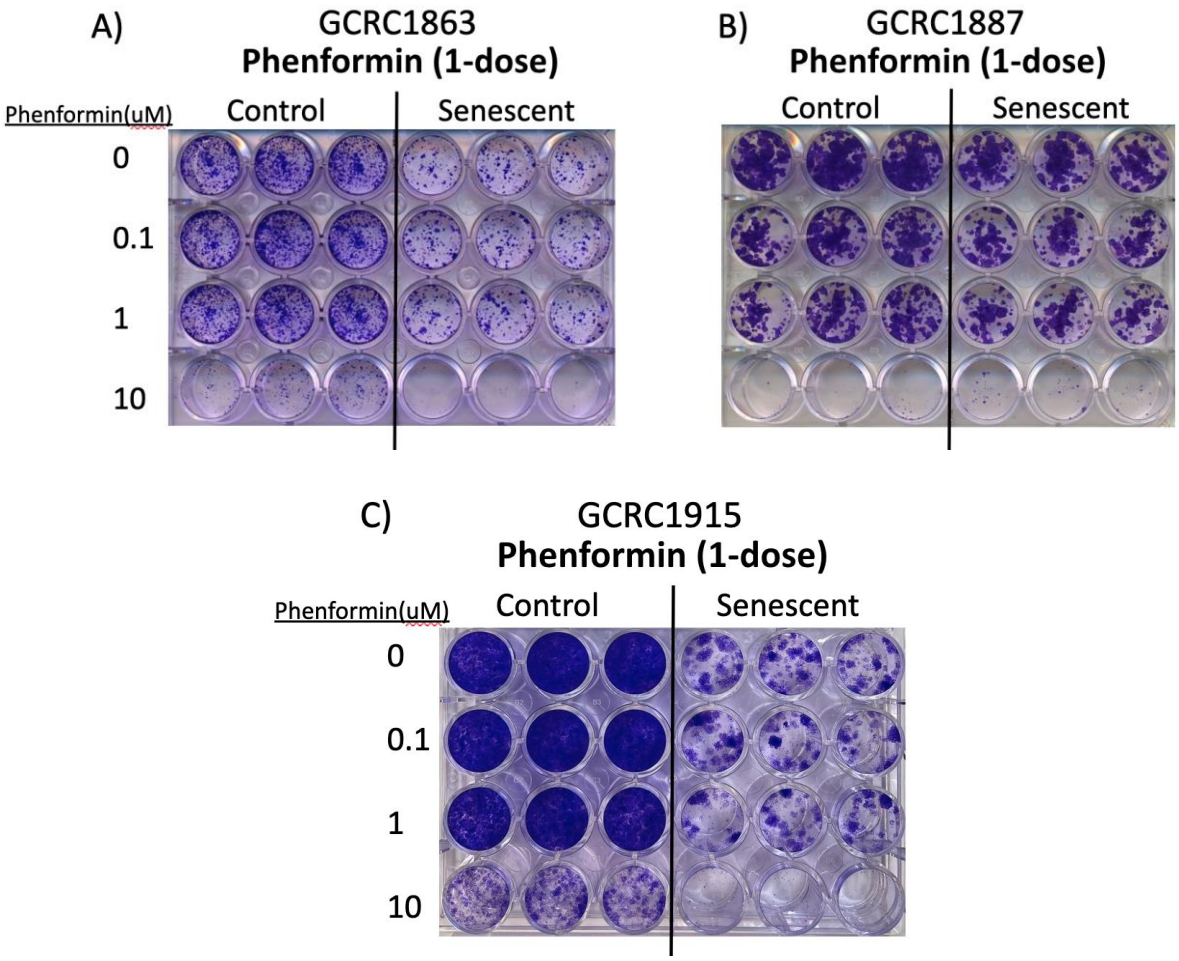
A)
GCRC1863
Phenformin (1-dose)
Phenformin(uM)
Control
Senescent
0
0.1
1
10
B)
GCRC1887
Phenformin (1-dose)
Control
Senescent
C)
GCRC1915
Phenformin (1-dose)
Phenformin(uM)
Control
Senescent
0
0.1
1
10

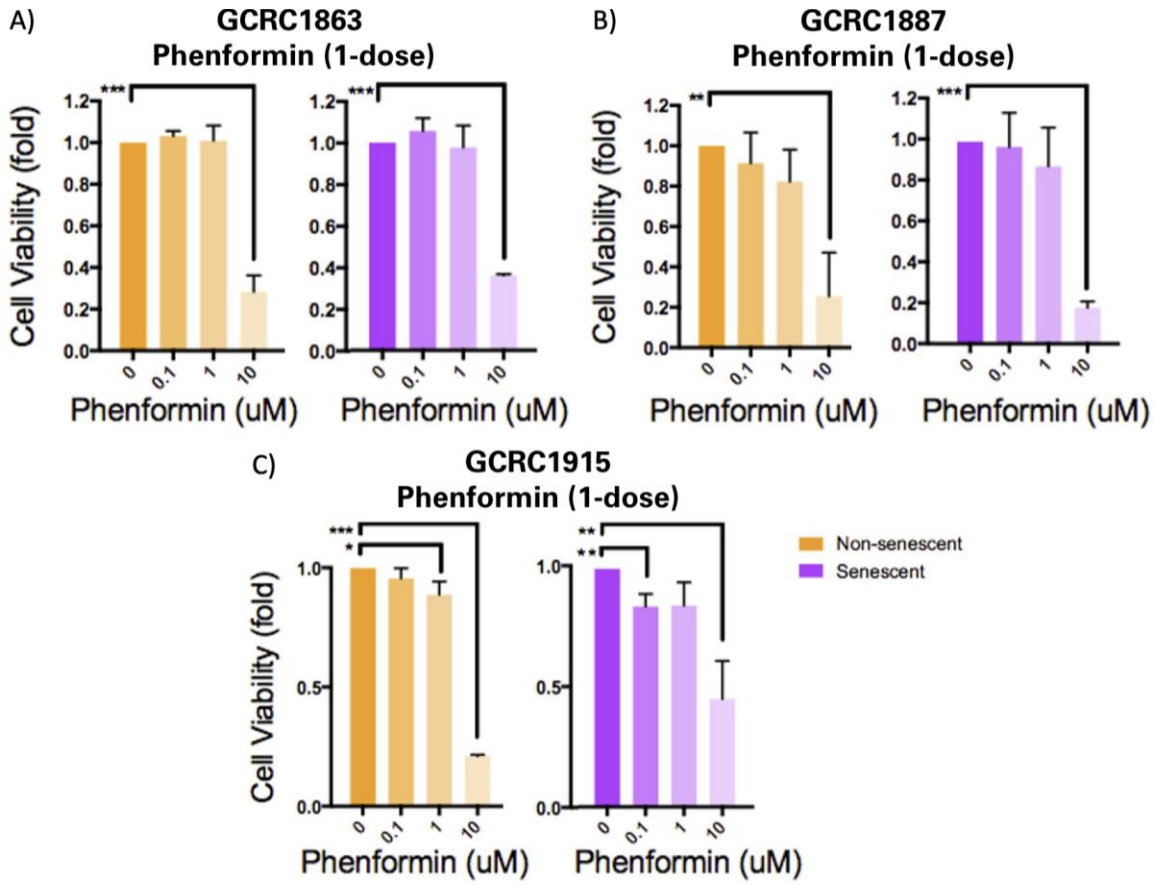

Figure 14. Clonogenic assays with the drug phenformin in PDX-derived breast cancer cell lines GCRC1863, GCRC1887, and GCRC1915. (A, B, C) GCRC1863, GCRC1887, or GCRC1915 cells were treated with phenformin on day 4 post-cisplatin treatment, and phenformin was removed from the cell culture media after 3 days. The plates were stained with 0.5% crystal violet staining solution. One asterisk represents $0.01 < \text{p-value} \leq 0.05$. Two asterisks represent $0.001 < \text{p-value} \leq 0.01$. Three asterisks represent $0.01 < \text{p-value} \leq 0.001$.

For all 3 primary breast cancer cell lines, high doses of phenformin (10 μM) were toxic to all cells irrespective of whether they were senescent. For both the GCRC1863 and GCRC1887 cell lines, cells given 0.1 μM or 1 μM phenformin proliferated at similar rates to control cells that were given no additional phenformin treatment (Fig. 14A, Fig. 14B). Overall, phenformin did not appear to be targeting senescent cells more selectively in both MDA-MB-231 cells and PDX-derived cell lines.

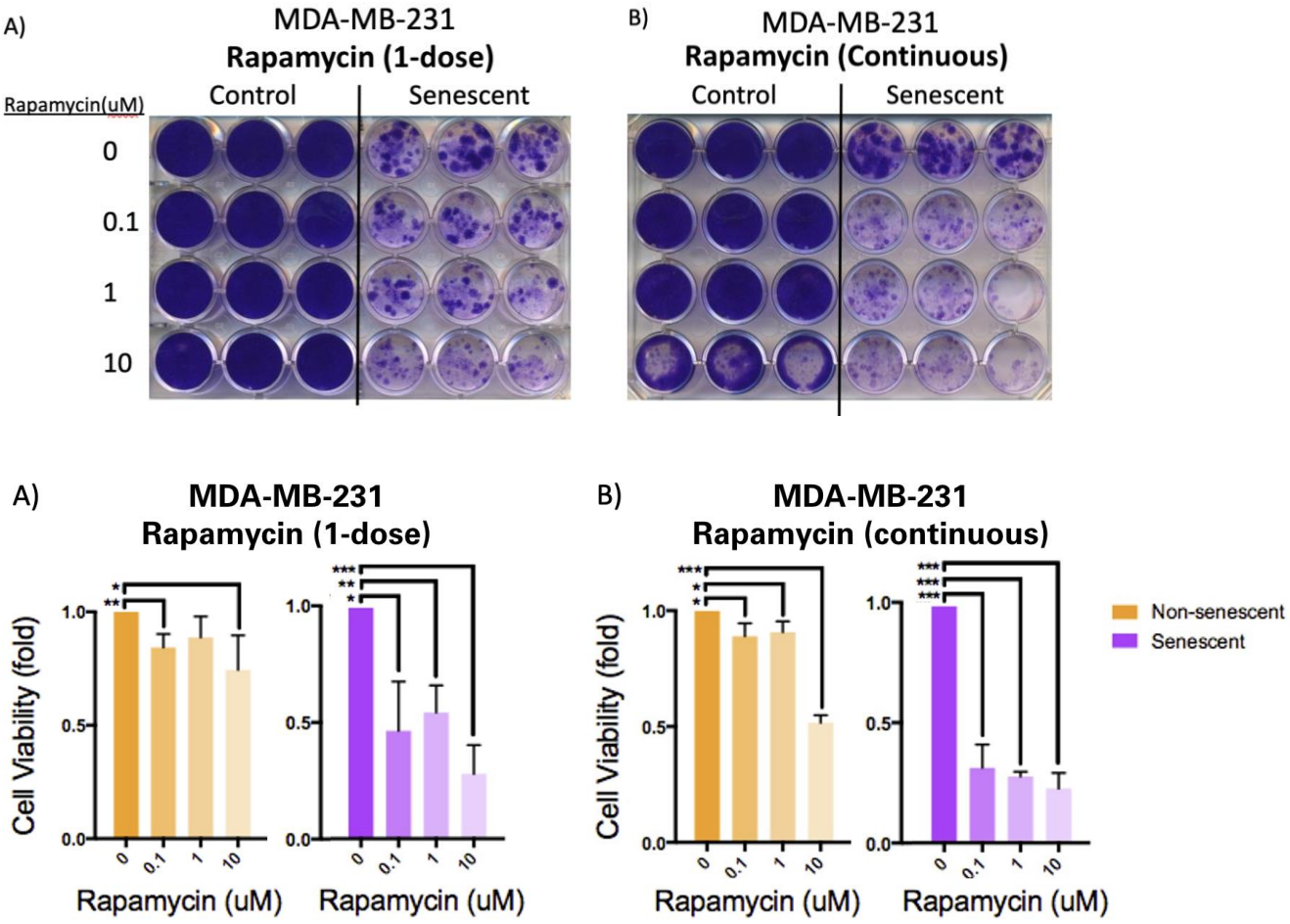

Figure 15. Clonogenic assays with the drug rapamycin administered once or continuously to MDA-MB-231 cells. (A) MDA-MB-231 cells were treated with rapamycin on day 4 post-cisplatin treatment, and rapamycin was removed from the culture media after 3 days. (B) MDA-MB-231 cells were treated continuously with the indicated dosage of rapamycin from day 4 post-cisplatin treatment until the experiment's endpoint. The plates were stained with 0.5% crystal violet staining solution. One asterisk represents $0.01 < \text{p-value} \leq 0.05$. Two asterisks represent $0.001 < \text{p-value} \leq 0.01$. Three asterisks represent $0.01 < \text{p-value} \leq 0.001$.

Senescent cells had significantly reduced cell viability in response to higher dosages of rapamycin (Fig. 15A), with a p-value < 0.01 for 1 μM rapamycin and a p-value < 0.001 for 10 μM rapamycin. When lower dosages of rapamycin (0.1 μM and 1 μM) were administered continuously to MDA-MB-231 cells, the senescent cell group had a more significant decrease in cell viability (p-values < 0.001) compared to the non-senescent group (Fig. 15B).

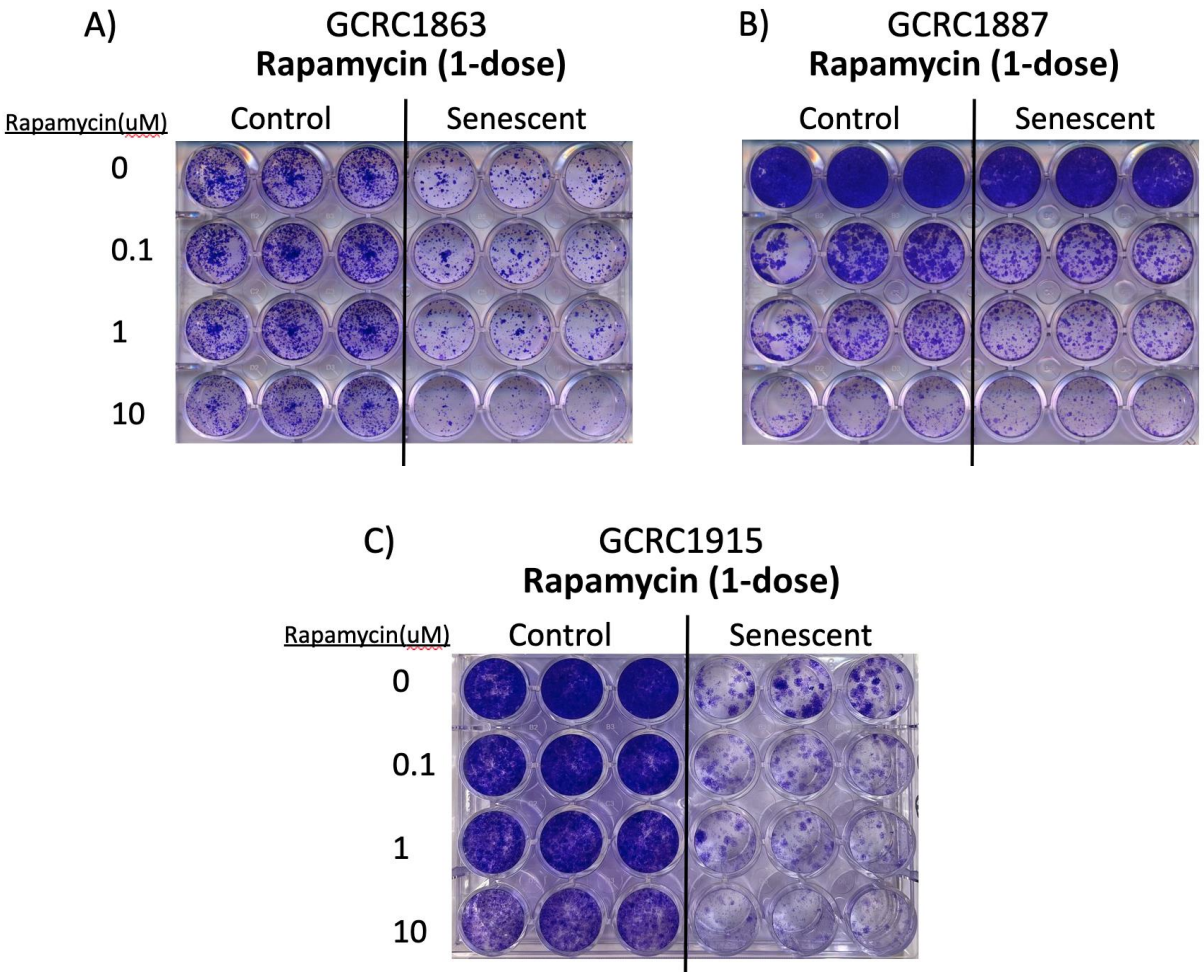
A)
GCRC1863
Rapamycin (1-dose)
Rapamycin(uM)
Control
Senescent
0
0.1
1
10
B)
GCRC1887
Rapamycin (1-dose)
Control
Senescent
C)
GCRC1915
Rapamycin (1-dose)
Rapamycin(uM)
Control
Senescent
0
0.1
1
10

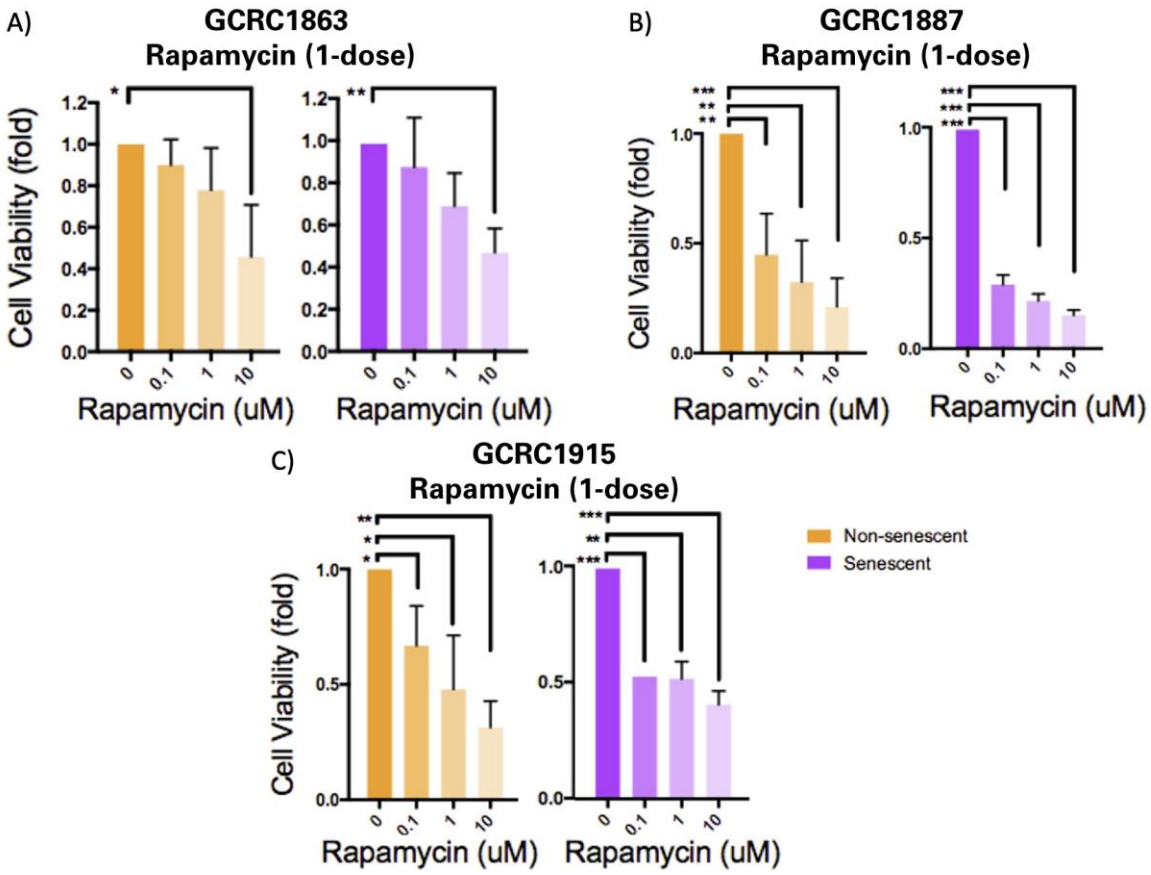

Figure 16. Clonogenic assays with the drug rapamycin in PDX-derived breast cancer cell lines GCRC1863, GCRC1887, and GCRC1915. (A, B, C) GCRC1863, GCRC1887, or GCRC1915 cells were treated with rapamycin on day 4 post-cisplatin treatment, and rapamycin was removed from the cell culture media after 3 days. The plates were stained with 0.5% crystal violet staining solution. One asterisk represents $0.01 < \text{p-value} \leq 0.05$. Two asterisks represent $0.001 < \text{p-value} \leq 0.01$. Three asterisks represent $0.01 < \text{p-value} \leq 0.001$.

For the GCRC1863 cell line, there is a more significant decline in cell viability among the senescent cell group in response to 10 μM of rapamycin (p-value < 0.01) compared to the control cell group. For the GCRC1887 cell line, rapamycin led to a more statistically significant decrease in cell viability (p-value < 0.001) among the senescent cell group than the control cell group when both groups were treated with 0.1 μM or 1 μM of rapamycin. Although mTOR has been implicated in cellular senescence, it is also involved in many other crucial cellular

processes, such as mitochondrial function, protein homeostasis, and immune response (79). Owing to its many roles in a cell, it remains unclear whether rapamycin selectively removes senescent cells.

4. Discussion and future directions

Most cells that are division-competent, including cancer cells, have demonstrated an ability to enter senescence upon induction (80). Our hypothesis was that senescence escape happens in the off-treatment periods and is partially responsible for the recurrence of the tumour following cancer treatment. To address the high rates of breast cancer relapse seen in patients with difficult-to-treat tumours, a one-two punch treatment regimen that eliminates the senescent cell population that remains after standard chemotherapy may have the potential to limit cancer regrowth following NACT.

In our preclinical model, senescence induction was confirmed in three ways: morphological changes, SA-β-gal staining, and protein expression levels. In cell culture, senescence is accompanied by morphological changes that can be easily visualized with a microscope—senescent cells become flattened and enlarged (81). This change in morphology was monitored over two weeks to confirm that senescence induction occurs following treatment with the chemotherapeutic agent cisplatin. MDA-MB-231 cells display the characteristic enlargement and flattening by day 3, and colonies resume their original proliferative morphology by day 7. For all the primary cancer cell lines, however, changes in cellular morphology are more prominent on day 7 post-cisplatin treatment. This may suggest that these primary cancer cells enter senescence later than MDA-MB-231 cells, perhaps attributable to the longer cell doubling time in primary cancer cells. By day 11 post-cisplatin, proliferating colonies with the same morphology as untreated cells can be seen in all the breast cancer cell lines. This is

consistent with the hypothesis that senescence escape occurs between chemotherapy rounds and contributes to cancer regrowth.

SA-β-gal activity was another biomarker used to confirm the presence of senescent cells in our preclinical model. Interestingly, breast cancer cells treated with 5 μM cisplatin for an hour showed comparable levels of senescence as cells that were treated with 40 μM cisplatin. This suggests that the extent to which cisplatin damages a cell's DNA within a short period of time may not correlate with its dosage. Thus, lower dosages of cisplatin could be combined with an additional senolytic to minimize the tumour in the neoadjuvant setting. Using lower dosages of cisplatin would reduce the side effects associated with its use.

There was a baseline level of senescence between the range of 10% to 20% seen in SA-β-gal staining in all the cell lines tested. The principal activator of senescence is DNA damage, which occurs spontaneously without external stressors (82). In normal physiological conditions, cellular senescence can also occur due to many reasons such as the shortening of the telomere, organelle damage, and epigenetic changes (83). Our finding that different cell lines have different baseline levels of senescence was another indicator of breast cancer's heterogeneity, as different cancers exhibit different levels of stress.

In our preclinical model, Lamin B1 levels decreased within 4 days after senescence induction with cisplatin and stayed low at day 7. This finding is consistent with other studies, which show that Lamin B1 expression declines rapidly within 48 hours after senescence induction from severe DNA damage (73). Since both SA-β-gal staining and a reduction in Lamin B1 expression are specifically observed in senescent cells and not quiescent cells, the induction of senescence through acute cisplatin exposure was confirmed in all four breast cancer cell lines.

Interestingly, p21 levels were only increased at day 4 for GCRC1887, but not on day 7. This observation can be explained by the fact that the induction of p21 in senescent cells is only transient; protein levels of p21 have been shown to decrease after cell cycle arrest has been established (76). Researchers have also observed a decrease in p53 levels after senescence induction, which further suggests that the p53/p21 pathway only regulates cellular senescence initiation (84). Our results are consistent with the finding from other researchers that senescence is a dynamic process in which different genes are expressed during its initiation versus maintenance.

However, the unexpected p21 levels could also be explained by the presence of p53 mutations in the breast cancer cells. The TP53 gene is truncated in GCRC1863 and harbors a missense mutation in GCRC1915 cells (68). As p21 is a target of p53, it depends on p53 activity (85). In cervix carcinoma cells, when levels of p53 were restored to normal levels, cells were more readily induced into senescence upon having DNA damage (86). TP53 gene is the most commonly mutated gene in a wide variety of human cancers, suggesting that perhaps many cancers harbor subtle perturbations that disrupt senescence and thus influence cancer susceptibility (87).

p16 is another biomarker of cellular senescence that could be used in place of p21 as a senescence indicator (88). Both p16 and p21 are CDK inhibitors that prevent cell cycle progression (89). Both the p53/p21 and p16/RB pathways are activated in senescence, and these two pathways appear to influence each other through many crosstalk mechanisms that have yet to be elucidated. Several studies have shown that p21 is mainly upregulated early during senescence induction, whereas p16 is involved in the maintenance of senescence (90). Evidence suggests that although p21 plays a role in initiating cell cycle arrest through CDK inactivation, all other hallmarks of senescence appear to occur independently of p21 activation (91). When

levels of p53 and p21 begin to decrease in senescent cells, p16 levels remained steadily high (92). When p53 becomes downregulated in senescent cells, Beausejour et al. demonstrated the importance of the p16/Rb pathway in directing senescent cells into one of two paths: re-proliferating or remaining in cell cycle arrest (93). Senescent cells escape senescence and replicate when p16 levels are low (93). If p16 levels stayed high, however, cells continue to be senescent (93). Researchers have shown that while senescence induction does not occur if p53 is inactivated prior to the increase in p16, once p16 is unregulated, inactivation of p53 at that point cannot reverse cell cycle arrest (94).

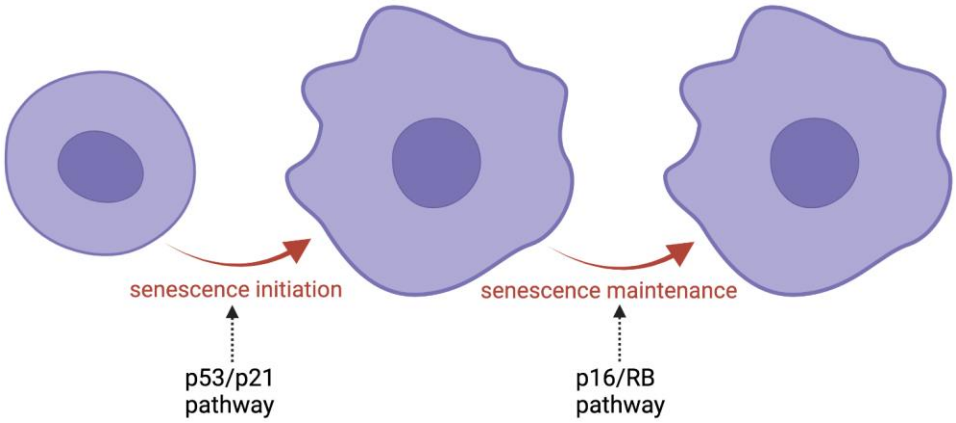

Figure 17. Both the p53/p21 and p16/RB pathways are activated in senescence, but at different time points. The p53/p21 pathway has been shown to be necessary for senescence induction, while the p16/RB pathway has been shown to keep cells in a senescent state. Created with BioRender.com.

Upon verifying that senescence induction occurred in our preclinical model, the potential of senolytics at preventing senescence escape was evaluated. The dose-response curves suggested that senescent breast cancer cells are more sensitive to the senolytic navitoclax than non-senescent cells. This demonstrated navitoclax's ability to selectively kill off senescent cells,

which suggests navitoclax may be an effective additional treatment following chemotherapy to limit senescence escape.

It was observed that chemotherapy-induced senescent MDA-MB-231 cells were selectively eliminated by one-time administration of the additional drugs navitoclax and rapamycin. Senolytics targeting proteins involved in anti-apoptotic pathways are shown to be more selective in this preclinical model, as anti-apoptotic pathways are significantly upregulated in senescent cells. In the PDX-derived breast cancer cell lines, there was a specific navitoclax concentration at which senescent cells were more selectively eliminated than non-senescent cells. This concentration differed among the primary cell lines, which proves the heterogeneous nature of breast cancer and suggests that different breast cancers respond differently to the same senolytic.

Notably, based on the morphological changes observed, PDX-derived breast cancer cells may develop the complete senescent phenotype later than MDA-MB-231 cells. The lack of senescent cells by day 3 post-cisplatin treatment may explain why the additional drugs administered were non-selective. Studies have shown that tumour cells develop a SASP more than 5 days after DNA damage of sufficient magnitude to induce senescence (95). This suggests that cells only fully develop all the characteristics associated with senescence, such as enlarged mitochondria, increased levels of free radicals, and protein aggregation in the endoplasmic reticulum, by day 5. It remains unclear whether the upregulation of anti-apoptotic pathways occurs before or after the other hallmarks of senescence take place, such as the release of SASP factors (96). The use of the broad-spectrum BCL-proteins inhibitor navitoclax would be the most effective at eliminating senescent cells when delivered after these cells' anti-apoptotic pathways become hyperactivated. It is plausible that PDX-derived breast cancer cells may develop the full

senescent phenotype later than MDA-MB-231 cells post cisplatin-treatment. If this is the case, it would be more effective to administer the additional senolytic at a later time point in the future.

Senolytic drugs face many challenges in terms of specificity and broad-spectrum activity against senescent cells due to the dynamic and heterogeneous nature of various types of senescence, which leads to the different types of senescent cells responding differently to senolytics (97). Through preventing cells from generating energy through oxidative phosphorylation, phenformin would theoretically eliminate senescent cells more selectively, since senescent cells rely more heavily on oxidative phosphorylation to sustain its metabolic activity. However, drugs that target the mitochondria of senescent cells are likely to also affect the metabolism of non-senescent cells, thereby eliminating all metabolically active cells. Much remains unknown about how the metabolism of senescent cells differs from non-senescent cells, so selective targeting of senescent cells' metabolic activity remains a challenge. This could explain why phenformin did not selectively eliminate senescent cells in any of the cell lines. SA-β-gal staining can detect diverse types of senescent cells, including chemotherapy-induced senescent cells (98). An increase in SA-β-gal staining was detected by day 3 following cisplatin treatment, which was why the additional senolytic was chosen to be administered to cells on day 4 post-cisplatin. These cells, although senescent, may not be targeted by phenformin in a specific manner. Non-selective activity would lead to serious side-effects if administered in vivo. To date, the most promising target of senolytics appears to be the pro-survival BCL-2 family proteins, as senescent cells must upregulate anti-apoptotic pathways to remain viable. It would be beneficial to identify additional compounds that could remove any growth-arrested cells remaining after chemotherapy rounds. CDK4/6 inhibition may be a potential target for limiting senescence escape and eventual cancer relapse due to its role in inducing cell cycle arrest by the p16/Rb pathway (99).

As senescence sometimes also serves a beneficial role, the therapeutic approach of clearing senescent tumour cells must be controlled to minimize the amount of non-tumour cells that are eliminated. Senescence is involved in embryonic development, wound healing from injuries, as well as host immunity through its SASP factors (100). As senescence provides clear benefits to the host, completely eliminating the ability of all cells to enter senescence may pose substantial problems from a clinical perspective. Even if a potent senolytic drug had very few off-target effects, the on-target toxicity could be formidable, such as by impairing wound healing in tissues. Impaired wound healing can be detrimental in older patients (100). Thus, rapamycin and phenformin, both of which have been extensively studied for their anticancer effects and inhibit pathways that are known to be upregulated in senescent cells, were chosen for the clonogenic assays.

In the future, the addition of senolytic drugs to prevent senescence escape would require further testing in animal models, which better mimics the biological progression of cancer growth. Since the rate at which cancer cells divide in vivo differs drastically from in vitro, it is likely that senescence induction as well as senescence escape occurs at a slower pace in-vivo. Since it is most effective to target cancer cells with an additional senolytic drug when they begin to show signs of senescence, it is necessary to determine the time point at which senescent markers begin to appear in vivo. However, because there are currently no biomarkers specific for senescence in vivo, there remains a critical need to identify any such biomarkers to identify senescent cells in vivo. Given the challenges of detecting senescent cells in vivo, it would also be challenging to measure the extent to which senolytics are eliminating senescent cells specifically.

5. Conclusions

This thesis established a preclinical model of senescence in breast cancer cells. These findings suggest that the timely administration of additional senolytic drugs to eliminate chemotherapy-induced senescent cells can significantly reduce breast cancer regrowth in vitro. In our preclinical model, the combination of cisplatin with selective senolytic drugs significantly reduced breast cancer survival and proliferation in the off-treatment periods. This suggests that NACT can be improved by incorporating additional drugs that target specific vulnerabilities of the cells that remain after chemotherapy. However, since current clinical strategies fall short in accurately identifying patients at high risk of recurrence, it is unfortunately very difficult to predict which patients may benefit more from additional treatment during NACT. Thus, the potential benefits of administering additional drugs in the NACT period must be balanced against the additional side effects it may bring upon patients. As cellular senescence participates in many complex physiological processes, we must better understand senescence to harness its benefits while repressing its tumour promoting effects.

References

1. Siegel, R. L., Miller, K. D., Fuchs, H. E. & Jemal, A. Cancer statistics, 2022. CA Cancer J Clin 72, 7-33, doi:10.3322/caac.21708 (2022).
2. Giaquinto, A. N. et al. Breast Cancer Statistics, 2022. CA Cancer J Clin 72, 524-541, doi:10.3322/caac.21754 (2022).
3. Ji, X. et al. Survival in Young Adults With Cancer Is Associated With Medicaid Expansion Through the Affordable Care Act. J Clin Oncol, JCO2201742, doi:10.1200/JCO.22.01742 (2022).
4. Canadian Cancer Society. Breast Cancer Statistics. Available from: https://cancer.ca/en/cancer-information/cancer-types/breast/statistics#:~:text=5%2C500%20Canadian%20women%20will%20die,from%20breast%20cancer%20every%20day.
5. Feng, Y. et al. Breast cancer development and progression: Risk factors, cancer stem cells, signaling pathways, genomics, and molecular pathogenesis. Genes Dis 5, 77-106, doi:10.1016/j.gendis.2018.05.001 (2018).
6. Colditz, G. A., Kaphingst, K. A., Hankinson, S. E. & Rosner, B. Family history and risk of breast cancer: nurses' health study. Breast Cancer Res Treat 133, 1097-1104, doi:10.1007/s10549-012-1985-9 (2012).
7. Hulka, B. S. Epidemiology of susceptibility to breast cancer. Prog Clin Biol Res 395, 159-174 (1996).
8. Collaborative Group on Hormonal Factors in Breast, C. Familial breast cancer: collaborative reanalysis of individual data from 52 epidemiological studies including 58,209 women with breast cancer and 101,986 women without the disease. Lancet 358, 1389-1399, doi:10.1016/S0140-6736(01)06524-2 (2001).

9. Kanbayashi, C. & Iwata, H. Current approach and future perspective for ductal carcinoma in situ of the breast. Jpn J Clin Oncol 47, 671-677, doi:10.1093/jjco/hyx059 (2017).
10. Cserni, G., Chmielik, E., Cserni, B. & Tot, T. The new TNM-based staging of breast cancer. Virchows Arch 472, 697-703, doi:10.1007/s00428-018-2301-9 (2018).
11. Park, M. et al. Breast Cancer Metastasis: Mechanisms and Therapeutic Implications. Int J Mol Sci 23, doi:10.3390/ijms23126806 (2022).
12. Pulido, C. et al. Bone metastasis risk factors in breast cancer. Ecancermedicalscience 11, 715, doi:10.3332/ecancer.2017.715 (2017).
13. Yin, L., Duan, J. J., Bian, X. W. & Yu, S. C. Triple-negative breast cancer molecular subtyping and treatment progress. Breast Cancer Res 22, 61, doi:10.1186/s13058-020-01296-5 (2020).
14. Riggio, A. I., Varley, K. E. & Welm, A. L. The lingering mysteries of metastatic recurrence in breast cancer. Br J Cancer 124, 13-26, doi:10.1038/s41416-020-01161-4 (2021).
15. Yersal, O. & Barutca, S. Biological subtypes of breast cancer: Prognostic and therapeutic implications. World J Clin Oncol 5, 412-424, doi:10.5306/wjco.v5.i3.412 (2014).
16. Dasari, S. & Tchounwou, P. B. Cisplatin in cancer therapy: molecular mechanisms of action. Eur J Pharmacol 740, 364-378, doi:10.1016/j.ejphar.2014.07.025 (2014).
17. Chen, S. H. & Chang, J. Y. New Insights into Mechanisms of Cisplatin Resistance: From Tumor Cell to Microenvironment. Int J Mol Sci 20, doi:10.3390/ijms20174136 (2019).
18. Ghosh, S. Cisplatin: The first metal based anticancer drug. Bioorg Chem 88, 102925, doi:10.1016/j.bioorg.2019.102925 (2019).

19. Spring, L. M. et al. Pathologic Complete Response after Neoadjuvant Chemotherapy and Impact on Breast Cancer Recurrence and Survival: A Comprehensive Meta-analysis. Clin Cancer Res 26, 2838-2848, doi:10.1158/1078-0432.CCR-19-3492 (2020).
20. Abdel-Razeq, H., Khalil, H., Assi, H. I. & Dargham, T. B. Treatment Strategies for Residual Disease following Neoadjuvant Chemotherapy in Patients with Early-Stage Breast Cancer. Curr Oncol 29, 5810-5822, doi:10.3390/curroncol29080458 (2022).
21. Weiss, A., Bashour, S. I., Hess, K., Thompson, A. M. & Ibrahim, N. K. Effect of neoadjuvant chemotherapy regimen on relapse-free survival among patients with breast cancer achieving a pathologic complete response: an early step in the de-escalation of neoadjuvant chemotherapy. Breast Cancer Res 20, 27, doi:10.1186/s13058-018-0945-7 (2018).
22. Zhu, M., Liang, C., Zhang, F., Zhu, L. & Chen, D. A Nomogram to Predict Disease-Free Survival Following Neoadjuvant Chemotherapy for Triple Negative Breast Cancer. Front Oncol 11, 690336, doi:10.3389/fonc.2021.690336 (2021).
23. Pan, H. et al. 20-Year Risks of Breast-Cancer Recurrence after Stopping Endocrine Therapy at 5 Years. N Engl J Med 377, 1836-1846, doi:10.1056/NEJMoa1701830 (2017).
24. Shahriari-Ahmadi, A., Arabi, M., Payandeh, M. & Sadeghi, M. The recurrence frequency of breast cancer and its prognostic factors in Iranian patients. Int J Appl Basic Med Res 7, 40-43, doi:10.4103/2229-516X.198521 (2017).
25. Lee Argov, E. J. et al. Breast cancer worry, uncertainty, and perceived risk following breast density notification in a longitudinal mammography screening cohort. Breast Cancer Res 24, 95, doi:10.1186/s13058-022-01584-2 (2022).

26. Gomis, R. R. & Gawrzak, S. Tumor cell dormancy. Mol Oncol 11, 62-78, doi:10.1016/j.molonc.2016.09.009 (2017).
27. Pedersen, R. N. et al. The Incidence of Breast Cancer Recurrence 10-32 Years After Primary Diagnosis. J Natl Cancer Inst 114, 391-399, doi:10.1093/jnci/djab202 (2022).
28. Tashima, Y. & Kawano, K. [A case of local recurrence developing thirty-nine years after mastectomy for breast cancer]. Gan To Kagaku Ryoho 41, 357-359 (2014).
29. Friberg, S. & Nystrom, A. Cancer Metastases: Early Dissemination and Late Recurrences. Cancer Growth Metastasis 8, 43-49, doi:10.4137/CGM.S31244 (2015).
30. Hayflick, L. & Moorhead, P. S. The serial cultivation of human diploid cell strains. Exp Cell Res 25, 585-621, doi:10.1016/0014-4827(61)90192-6 (1961).
31. Davalli, P. & Mitic, T. & Caporali, A. & Lauriola, A. & D'Arca, D. ROS, Cell Senescence, and Novel Molecular Mechanisms in Aging and Age-Related Diseases. Oxid Med Cell Longev 2016, 3565127, doi: 10.1155/2016/3565127 (2016).
32. Nagano, T. et al. Identification of cellular senescence-specific genes by comparative transcriptomics. Sci Rep 6, 31758, doi:10.1038/srep31758 (2016).
33. Maréchal, A. & Zou, L. DNA damage sensing by the ATM and ATR kinases. Cold Spring Harb Perspect Biol 5, 9 a012716, doi: 10.1101/cshperspect.a012716 (2013).
34. Brooks, C. L. & Gu, W. New insights into p53 activation. Cell Res 20, 614-621, doi:10.1038/cr.2010.53 (2010).
35. Abbas, T. & Dutta, A. p21 in cancer: intricate networks and multiple activities. Nat Rev Cancer 9, 400-414, doi:10.1038/nrc2657 (2009).
36. Rovillain, E., Mansfield, L., Lord, C. J., Ashworth, A. & Jat, P. S. An RNA interference screen for identifying downstream effectors of the p53 and pRB tumour suppressor

pathways involved in senescence. BMC Genomics 12, 355, doi:10.1186/1471-2164-12-355 (2011).

37. Neganova, I. & Lako, M. G1 to S phase cell cycle transition in somatic and embryonic stem cells. J Anat 213, 30-44, doi:10.1111/j.1469-7580.2008.00931.x (2008).
38. Macleod, K. F. The role of the RB tumour suppressor pathway in oxidative stress responses in the haematopoietic system. Nat Rev Cancer 8, 769-781, doi:10.1038/nrc2504 (2008).
39. Weidinger, A. & Kozlov, A. V. Biological Activities of Reactive Oxygen and Nitrogen Species: Oxidative Stress versus Signal Transduction. Biomolecules 5(2), 472-484, doi: 10.3390/biom5020472 (2015).
40. Calcinotto, A. et al. Cellular Senescence: Aging, Cancer, and Injury. Physiol Rev 99, 1047-1078, doi:10.1152/physrev.00020.2018 (2019).
41. Terzi, M. Y., Izmirli, M. & Gogebakan, B. The cell fate: senescence or quiescence. Mol Biol Rep 43, 1213-1220, doi:10.1007/s11033-016-4065-0 (2016).
42. Chan, A. S., Mowla, S. N., Arora, P. & Jat, P. S. Tumour suppressors and cellular senescence. IUBMB Life 66, 812-822, doi:10.1002/iub.1335 (2014).
43. Cuollo, L. & Antonangeli, F. & Santoni, A. & Soriani, A. The Senescence-Associated Secretory Phenotype (SASP) in the Challenging Future of Cancer Therapy and Age-Related Diseases. Biology (Basel) 9(12), 485, doi: 10.3390/biology9120485 (2020).
44. Greten, F. R. & Grivennikov, S. I. Inflammation and Cancer: Triggers, Mechanisms, and Consequences. Immunity 51, 27-41, doi:10.1016/j.immuni.2019.06.025 (2019).
45. Zhang, Y. et al. Cell Senescence: A Nonnegligible Cell State under Survival Stress in Pathology of Intervertebral Disc Degeneration. Oxid Med Cell Longev 2020, 9503562, doi:10.1155/2020/9503562 (2020).

46. Aird, K. M. & Zhang, R. Detection of senescence-associated heterochromatin foci (SAHF). Methods Mol Biol 965, 185-196, doi:10.1007/978-1-62703-239-1_12 (2013).
47. Zhang, R., Chen, W. & Adams, P. D. Molecular dissection of formation of senescence-associated heterochromatin foci. Mol Cell Biol 27, 2343-2358, doi:10.1128/MCB.02019-06 (2007).
48. Pagano, M., Pepperkok, R., Verde, F., Ansorge, W. & Draetta, G. Cyclin A is required at two points in the human cell cycle. EMBO J 11, 961-971, doi:10.1002/j.1460-2075.1992.tb05135.x (1992).
49. Coppe, J. P., Desprez, P. Y., Krtolica, A. & Campisi, J. The senescence-associated secretory phenotype: the dark side of tumor suppression. Annu Rev Pathol 5, 99-118, doi:10.1146/annurev-pathol-121808-102144 (2010).
50. Rodier, F. et al. Persistent DNA damage signalling triggers senescence-associated inflammatory cytokine secretion. Nat Cell Biol 11, 973-979, doi:10.1038/ncb1909 (2009).
51. Ozcan, S. et al. Unbiased analysis of senescence associated secretory phenotype (SASP) to identify common components following different genotoxic stresses. Aging (Albany NY) 8, 1316-1329, doi:10.18632/aging.100971 (2016).
52. Shimi, T. et al. The role of nuclear lamin B1 in cell proliferation and senescence. Genes Dev 25, 2579-2593, doi:10.1101/gad.179515.111 (2011).
53. Wang, A. S. & Ong, P. F. & Chojnowski, A. & Clavel, C. & Dreesen, O. Loss of Lamin B1 is a biomarker to quantify cellular senescence in photoaged skin. Sci Rep 7(1), 15678, doi: 10.1038/s41598-017-15901-9 (2017).

54. González-Gualda, E. et al. Galacto-conjugation of Navitoclax as an efficient strategy to increase senolytic specificity and reduce platelet toxicity. Aging Cell 19(4), e13142, doi: 10.1111/acel.13142 (2020).
55. Kale, J., Osterlund, E. J. & Andrews, D. W. BCL-2 family proteins: changing partners in the dance towards death. Cell Death Differ 25, 65-80, doi:10.1038/cdd.2017.186 (2018).
56. Geoghegan, F., Chadderton, N., Farrar, G. J., Zisterer, D. M. & Porter, R. K. Direct effects of phenformin on metabolism/bioenergetics and viability of SH-SY5Y neuroblastoma cells. Oncol Lett 14, 6298-6306, doi:10.3892/ol.2017.6929 (2017).
57. Papadopoli, D. et al. mTOR as a central regulator of lifespan and aging. F1000Res 8, doi:10.12688/f1000research.17196.1 (2019).
58. Weichhart, T. mTOR as Regulator of Lifespan, Aging, and Cellular Senescence: A Mini-Review. Gerontology 64, 127-134, doi:10.1159/000484629 (2018).
59. Pajak, B. et al. 2-Deoxy-d-Glucose and Its Analogs: From Diagnostic to Therapeutic Agents. Int J Mol Sci 21, doi:10.3390/ijms21010234 (2019).
60. Zhao, J. et al. Low-dose 2-deoxyglucose and metformin synergically inhibit proliferation of human polycystic kidney cells by modulating glucose metabolism. Cell Death Discov 5, 76, doi:10.1038/s41420-019-0156-8 (2019).
61. Aft, R. L., Zhang, F. W. & Gius, D. Evaluation of 2-deoxy-D-glucose as a chemotherapeutic agent: mechanism of cell death. Br J Cancer 87, 805-812, doi:10.1038/sj.bjc.6600547 (2002).
62. Michelakis, E. D., Webster, L. & Mackey, J. R. Dichloroacetate (DCA) as a potential metabolic-targeting therapy for cancer. Br J Cancer 99, 989-994, doi:10.1038/sj.bjc.6604554 (2008).

63. Tataranni, T. & Piccoli, C. Dichloroacetate (DCA) and Cancer: An Overview towards Clinical Applications. Oxid Med Cell Longev 2019, 8201079, doi:10.1155/2019/8201079 (2019).
64. Warburg, O. On the origin of cancer cells. Science 123, 309-314, doi:10.1126/science.123.3191.309 (1956).
65. Liberti, M. V. & Locasale, J. W. The Warburg Effect: How Does it Benefit Cancer Cells? Trends Biochem Sci 41, 211-218, doi:10.1016/j.tibs.2015.12.001 (2016).
66. Jenkins, D. E., Hornig, Y. S., Oei, Y., Dusich, J. & Purchio, T. Bioluminescent human breast cancer cell lines that permit rapid and sensitive in vivo detection of mammary tumors and multiple metastases in immune deficient mice. Breast Cancer Res 7, R444-454, doi:10.1186/bcr1026 (2005).
67. Panjehpour, M., Castro, M. & Klotz, K. N. Human breast cancer cell line MDA-MB-231 expresses endogenous A2B adenosine receptors mediating a Ca2+ signal. Br J Pharmacol 145, 211-218, doi:10.1038/sj.bjp.0706180 (2005).
68. Savage, P. et al. Chemogenomic profiling of breast cancer patient-derived xenografts reveals targetable vulnerabilities for difficult-to-treat tumors. Commun Biol 3, 310, doi:10.1038/s42003-020-1042-x (2020).
69. Fleury, H. et al. Exploiting interconnected synthetic lethal interactions between PARP inhibition and cancer cell reversible senescence. Nat Commun 10(1), 2556, doi: 10.1038/s41467-019-10460-1 (2019).
70. Mahmood, T. & Yang, P. C. Western blot: technique, theory, and trouble shooting. N Am J Med Sci 4, 429-434, doi:10.4103/1947-2714.100998 (2012).

71. Feoktistova, M., Geserick, P. & Leverkus, M. Crystal Violet Assay for Determining Viability of Cultured Cells. Cold Spring Harb Protoc 2016, pdb prot087379, doi:10.1101/pdb.prot087379 (2016).
72. West, R. Best practice in statistics: Use the Welch t-test when testing the difference between two groups. Ann Clin Biochem 58(4):267-269, doi: 10.1177/0004563221992088 (2021).
73. Freund, A., Laberge, R. M., Demaria, M. & Campisi, J. Lamin B1 loss is a senescence-associated biomarker. Mol Biol Cell 23, 2066-2075, doi:10.1091/mbc.E11-10-0884 (2012).
74. Dimri, G. P. et al. A biomarker that identifies senescent human cells in culture and in aging skin in vivo. Proc Natl Acad Sci U S A 92, 9363-9367, doi:10.1073/pnas.92.20.9363 (1995).
75. Debacq-Chainiaux, F., Erusalimsky, J. D., Campisi, J. & Toussaint, O. Protocols to detect senescence-associated beta-galactosidase (SA-betagal) activity, a biomarker of senescent cells in culture and in vivo. Nat Protoc 4, 1798-1806, doi:10.1038/nprot.2009.191 (2009).
76. Shtutman, M., Chang, B. D., Schools, G. P. & Broude, E. V. Cellular Model of p21-Induced Senescence. Methods Mol Biol 1534, 31-39, doi:10.1007/978-1-4939-6670-7_3 (2017).
77. Dotto, G. P. p21(WAF1/Cip1): more than a break to the cell cycle? Biochim Biophys Acta 1471, M43-56, doi:10.1016/s0304-419x(00)00019-6 (2000).
78. Jiang, X. & Kopp-Schneider, A. Summarizing EC50 estimates from multiple dose-response experiments: a comparison of a meta-analysis strategy to a mixed-effects model approach. Biom J 56, 493-512, doi:10.1002/bimj.201300123 (2014).

79. Iglesias-Bartolome, R. et al. mTOR inhibition prevents epithelial stem cell senescence and protects from radiation-induced mucositis. Cell Stem Cell 11, 401-414, doi:10.1016/j.stem.2012.06.007 (2012).
80. Rodier, F. & Campisi, J. Four faces of cellular senescence. J Cell Biol 192, 547-556, doi:10.1083/jcb.201009094 (2011).
81. Cho, K. A. et al. Morphological adjustment of senescent cells by modulating caveolin-1 status. J Biol Chem 279, 42270-42278, doi:10.1074/jbc.M402352200 (2004).
82. Di Micco, R., Krizhanovsky, V., Baker, D. & d'Adda di Fagagna, F. Cellular senescence in ageing: from mechanisms to therapeutic opportunities. Nat Rev Mol Cell Biol 22, 75-95, doi:10.1038/s41580-020-00314-w (2021).
83. Herranz, N. & Gil, J. Mitochondria and senescence: new actors for an old play. EMBO J 35, 701-702, doi:10.15252/embj.201694025 (2016).
84. Mijit, M., Caracciolo, V., Melillo, A., Amicarelli, F. & Giordano, A. Role of p53 in the Regulation of Cellular Senescence. Biomolecules 10, doi:10.3390/biom10030420 (2020).
85. Engeland, K. Cell cycle regulation: p53-p21-RB signaling. Cell Death Differ 29, 946-960, doi:10.1038/s41418-022-00988-z (2022).
86. Kapic, A. et al. Cooperation between p53 and p130(Rb2) in induction of cellular senescence. Cell Death Differ 13, 324-334, doi:10.1038/sj.cdd.4401756 (2006).
87. Beroukhim, R. et al. The landscape of somatic copy-number alteration across human cancers. Nature 463, 899-905, doi:10.1038/nature08822 (2010).
88. Rayess, H., Wang, M. B. & Srivatsan, E. S. Cellular senescence and tumor suppressor gene p16. Int J Cancer 130, 1715-1725, doi:10.1002/ijc.27316 (2012).
89. Besson, A., Dowdy, S. F. & Roberts, J. M. CDK inhibitors: cell cycle regulators and beyond. Dev Cell 14, 159-169, doi:10.1016/j.devcel.2008.01.013 (2008).

90. Buj, R., Leon, K. E., Anguelov, M. A. & Aird, K. M. Suppression of p16 alleviates the senescence-associated secretory phenotype. Aging (Albany NY) 13, 3290-3312, doi:10.18632/aging.202640 (2021).
91. Dulic, V., Beney, G. E., Frebourg, G., Drullinger, L. F. & Stein, G. H. Uncoupling between phenotypic senescence and cell cycle arrest in aging p21-deficient fibroblasts. Mol Cell Biol 20, 6741-6754, doi:10.1128/MCB.20.18.6741-6754.2000 (2000).
92. Helmbold, H., Komm, N., Deppert, W. & Bohn, W. Rb2/p130 is the dominating pocket protein in the p53-p21 DNA damage response pathway leading to senescence. Oncogene 28, 3456-3467, doi:10.1038/onc.2009.222 (2009).
93. Beausejour, C. M. et al. Reversal of human cellular senescence: roles of the p53 and p16 pathways. EMBO J 22, 4212-4222, doi:10.1093/emboj/cdg417 (2003).
94. Campisi, J. Senescent cells, tumor suppression, and organismal aging: good citizens, bad neighbors. Cell 120, 513-522, doi:10.1016/j.cell.2005.02.003 (2005).
95. Coppe, J. P. et al. Senescence-associated secretory phenotypes reveal cell-nonautonomous functions of oncogenic RAS and the p53 tumor suppressor. PLoS Biol 6, 2853-2868, doi:10.1371/journal.pbio.0060301 (2008).
96. Kirkland, J. L. & Tchkonia, T. Cellular Senescence: A Translational Perspective. EBioMedicine 21, 21-28, doi:10.1016/j.ebiom.2017.04.013 (2017).
97. Childs, B. G. et al. Senescent cells: an emerging target for diseases of ageing. Nat Rev Drug Discov 16, 718-735, doi:10.1038/nrd.2017.116 (2017).
98. Cai, Y. et al. Elimination of senescent cells by beta-galactosidase-targeted prodrug attenuates inflammation and restores physical function in aged mice. Cell Res 30, 574-589, doi:10.1038/s41422-020-0314-9 (2020).

99. Wagner, V. & Gil, J. Senescence as a therapeutically relevant response to CDK4/6 inhibitors. Oncogene 39, 5165-5176, doi:10.1038/s41388-020-1354-9 (2020).

100. He, S. & Sharpless, N. E. Senescence in Health and Disease. Cell 169, 1000-1011, doi:10.1016/j.cell.2017.05.015 (2017).